ERDC/GSL TR-07-18

Geotechnical and Structures Laboratory

US Army Corps
of Engineers®
Engineer Research and
Development Center

Evaluation Criteria for Aged Asphalt Concrete Surfaces

Haley P. Bell and Reed B. Freeman

June 2007

ERDC/GSL TR-07-18
June 2007

Evaluation Criteria for Aged Asphalt Concrete Surfaces

Haley P. Bell and Reed B. Freeman

Geotechnical and Structures Laboratory
U.S. Army Engineer Research and Development Center
3909 Halls Ferry Road
Vicksburg, MS 39180-6199

Final report

Prepared for Headquarters, Air Force Civil Engineer Support Agency
139 Barnes Avenue, Suite 1
Tyndall AFB, FL 32403-5319

Abstract: An evaluation of aged asphalt concrete (AC) was performed during the period February to December 2006 at the Vicksburg Airport (Vicksburg, MS), Hood Army Airfield and Robert Gray Army Airfield (Fort Hood, TX), Lawson Army Airfield (Fort Benning, GA), Cairns Army Airfield (Fort Rucker, AL), Butts Army Airfield (Fort Carson, CO), and Kandahar Airfield (Kandahar, Afghanistan) to develop a method for predicting the performance of aged AC surfaces in situ. A portable seismic pavement analyzer (PSPA) was used on the in situ AC pavements to determine the pavement modulus. The aged AC samples obtained from the military airfields were brought to the U.S. Army Engineer Research and Development Center for further laboratory testing. Various asphalt mixture and binder properties were determined from the samples, indirect tensile strength tests were run on core samples, and beam fatigue tests were performed on beam samples. The results from this study were used to develop adjustments to the current Department of Defense (DoD) fatigue criterion for the purpose of improving fatigue life predictions for aged AC surfaces. Aged AC surfaces are considered to be 10 years old or older. The most accurate adjustment to the current DoD criterion required both asphalt modulus (from PSPA) and binder stiffness (from dynamic shear rheometer) as input.

Contents

Figures and Tables

Figures

Tables

Preface

The project described in this report was sponsored by Headquarters, Air Force Civil Engineer Support Agency, Tyndall Air Force Base, FL.

Personnel of the U.S. Army Engineer Research and Development Center, Geotechnical and Structures Laboratory (GSL), Vicksburg, MS, prepared this publication. The findings and recommendations presented in this report are based upon evaluations of aged asphalt concrete pavements from the Vicksburg Municipal Airport in Vicksburg, MS, Hood Army Airfield and Robert Gray Army Airfield in Fort Hood, TX, Lawson Army Airfield in Fort Benning, GA, Cairns Army Airfield in Fort Rucker, AL, Butts Army Airfield in Fort Carson, CO, and Kandahar Airfield in Kandahar, Afghanistan. The required field testing was conducted during the period February to October 2006, and the laboratory testing was conducted during March to December 2006.

The evaluation team consisted of Haley P. Bell, Chase T. Bradley, Roosevelt Felix, Jr., Jason G. Knox, and Ernest Woodward, all of the Airfields and Pavements Branch (APB), GSL. Mrs. Bell and Dr. Reed B. Freeman, APB, prepared this publication under the supervision of Don R. Alexander, Chief, APB; Dr. Larry N. Lynch, Acting Chief, Engineering Systems and Materials Division; Dr. William P. Grogan, Deputy Director, GSL; and Dr. David W. Pittman, Director, GSL.

COL Richard B. Jenkins was Commander and Executive Director of ERDC. Dr. James R. Houston was Director.

Recommended changes for improving this publication in content and/or format should be submitted on DA Form 2028 (Recommended Changes to Publications and Blank Forms) and forwarded to Headquarters, U.S. Army Corps of Engineers, ATTN: CECW-EW, 441 G Street NW, Washington, DC 20314.

Unit Conversion Factors

Multiply	By	To Obtain
degrees Fahrenheit	(F-32)/1.8	degrees Celsius
feet	0.3048	meters
inches	0.0254	meters
kips (force) per square inch	6.894757	megapascals
pounds (force) per square inch	6.894757	kilopascals
pounds (mass)	0.45359237	kilograms

Summary

Personnel of the U.S. Army Engineer Research and Development Center (ERDC), Vicksburg, MS, conducted an evaluation of aged asphalt concrete (AC) surfaces during February to December 2006 in order to determine a method for predicting pavement performance. Field testing took place at the Vicksburg Municipal Airport, Vicksburg, MS; Hood Army Airfield and Robert Gray Army Airfield, Fort Hood, TX; Lawson Army Airfield, Fort Benning, GA; Cairns Army Airfield, Fort Rucker, AL; and Butts Army Airfield, Fort Carson, CO. The in situ surface modulus of the AC samples was determined using a portable seismic pavement analyzer (PSPA). Samples of the aged AC were removed from the airfields and brought to the ERDC asphalt laboratory where indirect tensile strength (ITS) tests (ASTM D 6931-07) and beam fatigue tests were conducted. Furthermore, various asphalt mixture and binder properties were determined from the samples.

Two additional samples were evaluated using the same procedure described previously. One sample was from Kandahar International Airport in Kandahar, Afghanistan, which is a location in the theater of operations where premature AC deterioration was reported. The other sample consisted of a high-quality AC airfield mix prepared in the ERDC asphalt laboratory.

The results of the tests and evaluation reveal the following:

a. In a laboratory study intended to validate methods by which the PSPA is used for Department of Defense (DoD) pavement evaluations, the AC design modulus equation (shown below) that is used to adjust the modulus measured by the PSPA to a temperature of 77°F and a standard design frequency of 15 Hz, appears to provide reasonable results for aged AC pavements.

$$E_{77^{o}F} = \frac{E_{PSPA}}{\left(\left\{-0.0109 * \left[(T-32) * \frac{5}{9}\right] + 1.2627\right\} * (3.2)\right)}$$

$E_{77°F}$ = AC design modulus, ksi
E_{PSPA} = modulus measured by the PSPA, ksi

T = AC pavement temperature, ˚F

b. In the laboratory validation study mentioned above, PSPA results detected softening of aged AC pavements at a high temperature of 120˚F, but did not detect a difference between the moduli of aged AC pavements between the temperatures of 40 and 75°F. This was attributed to the overriding effect of AC aging.

c. The current DoD criterion for AC fatigue life, which was developed using laboratory-produced beam samples, predicts fatigue life as a function of AC modulus and tensile strain (or tensile stress). The current DoD criterion has difficulty predicting fatigue failure for aged AC samples (10 years or older) obtained from the field. Results from this study indicate that, in some cases, the error in this prediction can be highly unconservative; that is, predicted cycles to failure were much higher than measured cycles to failure.

d. A method for adjusting the current DoD fatigue criterion to better predict aged AC failure was developed and can be applied to various strain levels and AC moduli. In this study, the developments toward a new criterion were limited to "adjusting" the current criterion because beam fatigue tests were limited to only one strain level (550 microstrains). Results from this study support the need to develop a fatigue criterion for aged AC that is independent of the current DoD criterion. This is best accomplished by conducting beam fatigue tests at various strain levels.

e. AC modulus, as measured by the PSPA, provided the best single material parameter for improving the predictive capability of the current DoD fatigue criterion. AC modulus was found to be an important parameter for "adjusting" the current DoD fatigue criterion because the effect of modulus on fatigue life is diminished for aged AC, relative to its effects for laboratory-produced asphalt. In other words, modulus was important for the criterion "adjustment" because the net effect of the adjustment was to remove the influence of modulus as an independent predictive variable.

f. The only other material parameter that, when used by itself, offered a significant contribution to adjusting the current DoD fatigue criterion was the peak strength value of the ITS test. This parameter was able to

eliminate cases in which predicted fatigue life was much higher than measured fatigue life, but overall accuracy of fatigue predictions was not improved substantially. The effectiveness of the ITS parameter was facilitated by its relatively high, positive correlation with PSPA modulus.

g. The most preferred method for adjusting the current DoD fatigue criterion involved the use of both PSPA modulus and a viscoelastic binder stiffness property ($G^*/(\sin \delta)$) that was obtained from dynamic shear rheometer (DSR) testing. The authors hypothesize that the effectiveness of this combination is related to the consideration of both mixture and binder properties, as provided by the PSPA and DSR, respectively.

h. AC age, various AC mixture parameters, ITS energy to peak strength, and ITS compression at peak strength showed poor contributions toward adjusting the current DoD asphalt fatigue criterion for the purpose of improved predictions of fatigue life for aged AC pavements.

Until further testing and analysis are conducted using varying strain levels, the following recommendations are offered based upon the results of the field and laboratory testing of aged AC pavements:

a. When evaluating aged AC surfaces with the PSPA, use the standard AC design modulus equation (shown below) for converting moduli to "standard" moduli at 77°F and 15 Hz.

$$E_{77^{\circ}F} = \frac{E_{PSPA}}{\left(\left\{-0.0109 * \left[(T-32) * \frac{5}{9}\right] + 1.2627\right\} * (3.2)\right)}$$

$E_{77°F}$ = AC design modulus, ksi
E_{PSPA} = modulus measured from the PSPA, ksi
T = AC pavement temperature, °F

b. The PSPA can give erroneous results when its contact with the pavement is poor and when surface distresses affect the travel of energy waves. Therefore, the pavement evaluation team needs to ensure that at least three test repetitions are measured at each location and at least ten PSPA measurements are obtained for each pavement feature.

c. Use the following equation to predict aged AC performance if elastic modulus is the only data available:

$$\varepsilon_r = 10^{(X_{aged})}$$

$$X_{aged} = -7.1682 - 5.0 * Log\, S_A - 2.665 * Log\, E + 0.0028 * E$$

ε_r = allowable strain repetitions
S_A = tensile strain of AC, in./in.
E = elastic modulus of AC, ksi

d. Use the following equation to predict aged AC (10+ years) performance if both elastic modulus and G*/(sin δ) data are available:

$$\varepsilon_r = 10^{(X_{aged})}$$

$$X_{aged} = -6.7328 - 5.0 * Log\, S_A - 2.665 * Log\, E + 0.0025 * E - 6.7663 * (G^* / sin\delta)$$

ε_r = allowable strain repetitions
S_A = tensile strain of AC, in./in.
E = elastic modulus of AC, ksi
$G^*/(sin\ \delta)$ = binder stiffness obtained from a DSR, MPa

Among the two proposed adjusted criteria, this is the preferred equation because it proved to be the most accurate method for predicting fatigue life in this study.

e. If the strain at the bottom of the AC is unknown, then refer to Tables 19 and 20 in Chapter 4 for typical values of S_A according to DoD aircraft, AC thickness, AC modulus, and aircraft pass levels. The values of S_A can be used in the equations for predicting aged AC performance.

Chapter 1 of this report presents the objective and scope of the project, and Chapter 2 discusses the field procedures including a description of the test sites. Chapter 3 summarizes the laboratory testing procedures and presents the results of the laboratory tests. Chapter 4 summarizes the data

analysis and findings from the evaluation, and Chapter 5 provides the conclusions and recommendations based on information gained from the aged AC surface evaluation.

1 Introduction

Background

The Air Force Civil Engineer Support Agency (AFCESA) pavement evaluation teams are under constant pressure to provide accurate field assessments of pavement load-carrying capacity. Pavement evaluation results provide critical information needed by major command engineers for mission planning and optimization of rehabilitation strategies. The AFCESA has an immediate need for testing and analytical procedures for assessing the integrity of asphalt concrete (AC) surface layers and predicting the performance of aged AC when subjected to heavy wheel loads and high tire pressures.

Many times, in military operations, it is necessary to use existing airfields or roads that consist of aged or brittle AC surfaces. The U.S. Air Force's ability to select suitable operating surfaces in the theater of operation is limited by the current methods being used for the visual and structural evaluation of AC pavements, which have failed to identify problems caused by the use of such pavements. If the airfield pavement evaluation indicates adequate load-carrying capacity using current procedures, but then a sudden increase in traffic volume and loading causes the aged AC pavements to fail prematurely due to severe cracking and an increase in foreign object debris (FOD), the mission will be severely impacted. The mission will be impacted because of the additional time and efforts required to sustain operations, restricted operations due to repair requirements, additional damage to aircraft due to the high FOD, and a drain on engineering resources leading to reduced availability. Future military missions may be severely impacted without the ability to predict the performance of aged AC pavements accurately.

Objective and scope

The purpose of this research was to address issues with evaluating and predicting the performance of deteriorated AC surfaces. In order to accomplish this, several aged AC samples were located and evaluated. The evaluation consisted of determining the in situ AC modulus using the portable seismic pavement analyzer (PSPA), determining the strength of the samples using indirect tensile strength (ITS) testing, measuring various

mixture and binder properties of the aged samples, and determining the fatigue life of the AC using beam fatigue tests. The primary objective of this investigation was to determine a methodology for evaluating aged AC surfaces on existing paved surfaces. This report provides data for the following:

a. Visually inspecting aged AC surfaces on various airfields

b. Completing field testing that can be used to identify and quantify parameters for evaluating the fatigue performance of aged AC surfaces

c. Completing laboratory testing of samples removed from the aged AC surfaces

d. Conducting an analysis of any pavement system having an aged AC surface.

This report provides field and laboratory testing procedures, data analysis, and recommendations for evaluating and predicting the performance of aged AC surfaces.

2 Field Procedures

Description of test sites

The evaluation of aged AC began in February 2006 at the Vicksburg Municipal Airport in Vicksburg, MS, and Hood Army Airfield and Robert Gray Army Airfield in Fort Hood, TX, in March 2006. Field testing continued in April 2006 at Cairns Army Airfield in Fort Rucker, AL, and Lawson Army Airfield in Fort Benning, GA, and concluded in May 2006 at Butts Army Airfield in Fort Carson, CO. Further investigations, including the laboratory testing, began in March 2006 and concluded in December 2006. Figure 1 shows the geographical locations of the test sites. Thirteen aged AC samples were obtained from these locations (Table 1).

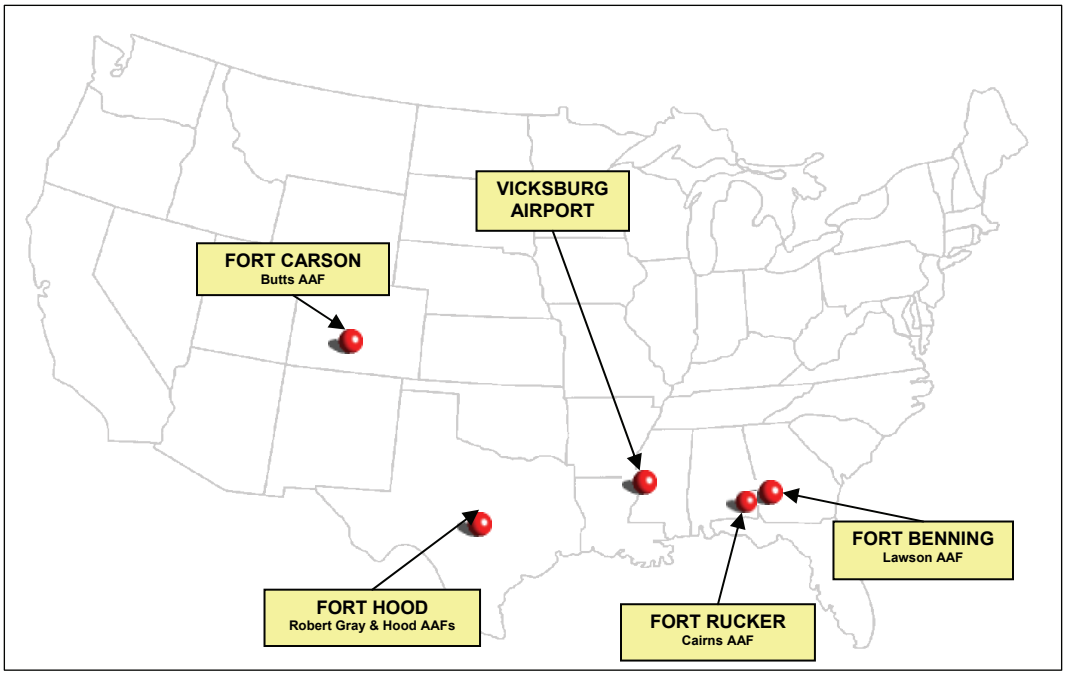

Figure 1. Test site locations.

An additional sample was obtained in November 2006 from Kandahar International Airport in Kandahar, Afghanistan. Kandahar Airfield is a location in the theater of operations where premature AC deterioration was reported.

A high-quality standard airfield mix AC sample (AC-30) was prepared in the Engineer Research and Development Center (ERDC) asphalt

Table 1. Sample nomenclature and description.

Sample	Description	Airfield Location	Age (yr)
VA-3	Vicksburg Municipal Airport	Apron	41
H-1	Hood Army Airfield	Runway End	25
H-2	Hood Army Airfield	Taxiway	19
H-3	Hood Army Airfield	Apron	35
RG-1	Robert Gray Army Airfield	Apron	19
RG-2	Robert Gray Army Airfield	Apron	55
L-1	Lawson Army Airfield	Taxiway	46
L-2	Lawson Army Airfield	Taxiway	46
C-1	Cairns Army Airfield	Apron	31
C-2	Cairns Army Airfield	Apron	50
B-1	Butts Army Airfield	Taxiway	5
B-2	Butts Army Airfield	Taxiway	38
B-3	Butts Army Airfield	Runway Turnaround	38
KA-1	Kandahar Airfield	Taxiway	30
LM	Lab Mix	--	0

laboratory in October 2006. This mix was produced to conform to both UFC 3-25-03 (“Standard Practice Manual for Flexible Pavements”) and UFGS-02749 (“Hot-Mix Asphalt (HMA) for Airfields”). The sample was prepared in a portable pug mill mixer and formed in a steel frame as shown in Figure 2. Figure 3 shows the sample being compacted, and Figure 4 shows the formed and compacted laboratory mix sample. The purpose of the laboratory prepared sample was to use it as a basis of comparison for the aged AC samples.

Figure 5 shows the layout used for sawing cylinders and beams from each field sample. Two to three samples were obtained from each site. The samples were approximately 2 ft by 3 ft and at least 3 in. thick. This produced four beams for beam fatigue testing and three 4-in.-diam cores for ITS testing. The 14-in. by 24-in. section shown in Figure 5 was used for obtaining various mixture and binder properties of the AC samples.

Figures 6 through 9 illustrate the basic procedure for field testing, removal of the aged AC samples, and pavement repair. Each sample was tested with the PSPA before it was removed from the airfield to obtain the in situ modulus of the AC. The PSPA was not accessible when the KA-1 sample

Figure 2. Pouring the laboratory mix sample in the frame.

Figure 3. Compacting the laboratory mix sample.

Figure 4. Formed and compacted laboratory mix sample.

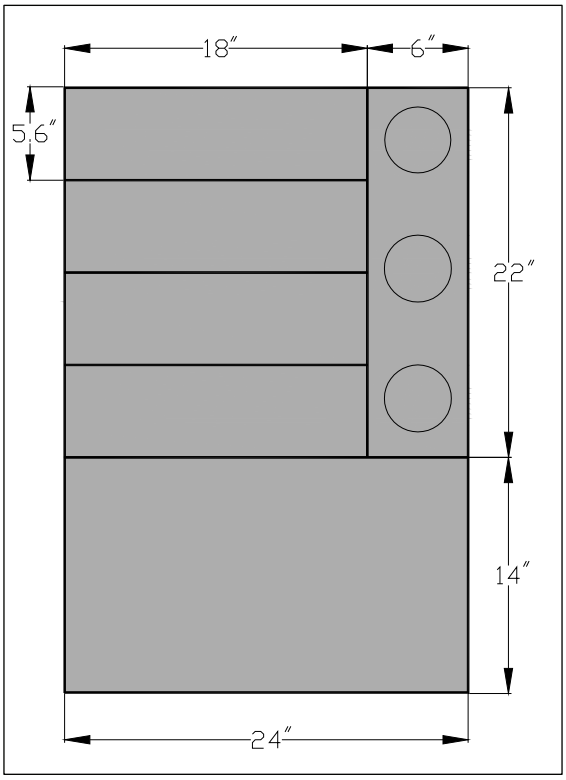

Figure 5. Sample layout.

Figure 6. Obtaining the in situ modulus using the PSPA.

Figure 7. Sawing the aged AC sample.

Figure 8. Removing the aged AC sample.

Figure 9. Patching the hole of the removed aged AC sample.

was removed from Kandahar Airfield; however, the KA-1 sample and the LM sample were tested with the PSPA in the ERDC asphalt laboratory prior to the removal of the beams and cores. Generally, as shown in Figure 7, cores were extracted on site and the beams were sawn in the laboratory. Once the in situ modulus was obtained with the PSPA and the cores were extracted, the sample was sawed and removed, and the hole was patched.

Portable seismic pavement analyzer tests

The PSPA (Figure 10), developed by Geomedia Research and Development in El Paso, TX, is a nondestructive device that rapidly measures Young's modulus via ultrasonic surface waves, completing tests within a few seconds. The PSPA is used to estimate the in situ seismic modulus of concrete pavements and determine relevant strength parameters for use in pavement evaluations such as those conducted by the Department of Defense (DoD) in accordance with the Unified Facilities Criteria 3-260-03 (Headquarters, Departments of the Army, the Navy, and the Air Force 2001a).

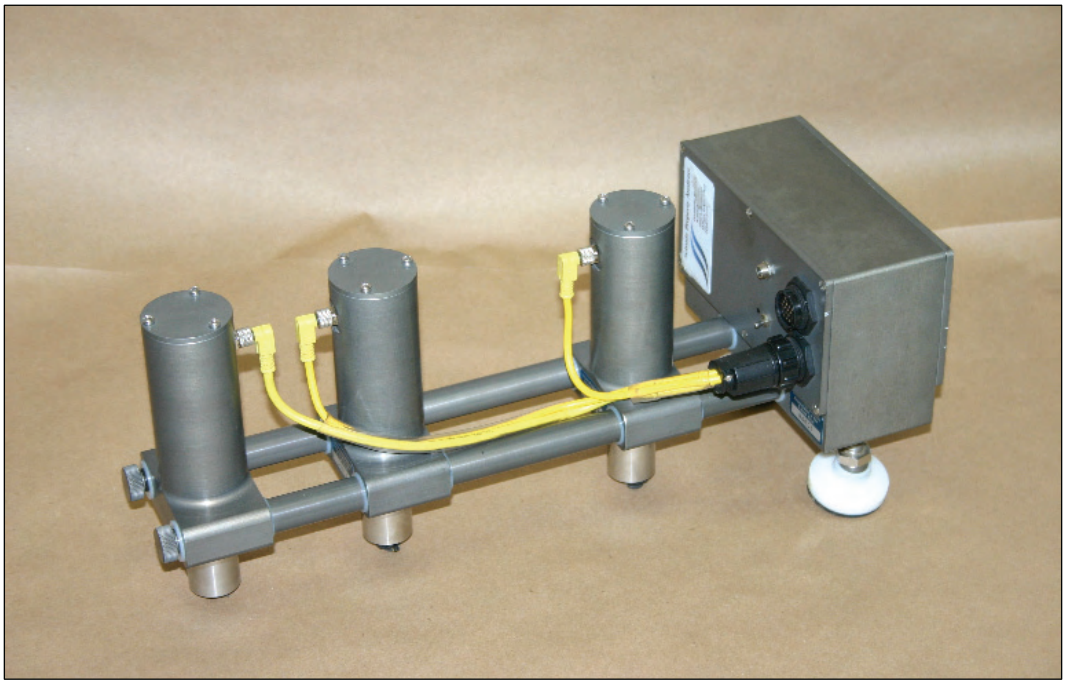

Figure 10. Portable seismic pavement analyzer (PSPA).

The PSPA was included in this study because of its simplicity and ease of use for determining in situ surface modulus. The device is operated from a laptop computer, which is connected to an electronics box by a cable that transmits power to the receivers and the source. The source impacts the

pavement surface, generating surface waves that are detected by the receivers. The measured signals are returned to the data acquisition board in the computer. The velocity at which the surface waves propagate is determined, and the modulus is computed.

For this study, the PSPA was used to measure the modulus of the aged AC samples before they were removed from the airfields. An average modulus for each sample was determined by conducting three to five PSPA tests at the same location. The modulus of AC pavements is dependent upon temperature; therefore, a design modulus must be used to standardize the PSPA results for purposes of predicting pavement performance. The AC design modulus is used to adjust the modulus measured by the PSPA to a temperature of 77°F and a design frequency of 15 Hz using Equation 1 (Nazarian et al. 2005).

$$E_{77^{o}F} = \frac{E_{PSPA}}{\left(\left\{-0.0109 * \left[(T-32) * \frac{5}{9}\right] + 1.2627\right\} * (3.2)\right)} \quad (1)$$

$E_{77°F}$ = AC design modulus, ksi
E_{PSPA} = modulus measured from the PSPA, ksi
T = AC pavement temperature, °F

The AC design modulus is incorporated with the test results during the data analysis phase. $E_{77°F}$ is the adjusted AC modulus value to use for recording or analyzing. Table 2 shows the in situ modulus values (both measured with the PSPA and adjusted using Equation 1) of the AC samples. These data were obtained before the samples were removed from the airfield.

Table 2. Field PSPA modulus values.

Sample	Temperature (°F)	PSPA Modulus (ksi)	AC Design Modulus (ksi)
VA-3	75	1953	609
H-1	65	2023	595
H-2	90	2305	790
H-3	105	1817	692
RG-1	60	2030	580
RG-2	65	2928	861
L-1	52	978	268
L-2	73	2000	616
C-1	95	2745	973
C-2	95	2193	778
B-1	72	1368	419
B-2	91	1514	523
B-3	92	1438	500

3 Laboratory Procedures

Asphalt properties

Mixture properties

Mixture properties (density, AC content, and gradation) of the aged AC samples were measured to validate results from the strength tests and explain pavement behavior or variability in the data. The density, or rice gravity (ASTM D 2041-03a), gives the maximum theoretical mix specific gravity of the uncompacted bituminous paving mixture at 77°F. Extractions (ASTM D 2172-05) give a quantitative measure of bitumen in the aged AC samples. The higher the value of extraction, the more asphalt content in the aged AC sample. For this test, the aggregate is extracted from the AC mixture and used for the gradation tests. Gradation (ASTM C 136-06) is the particle size distribution of fine and coarse aggregates by sieve analysis. The coarse aggregates were defined as the percent of the sample that was retained on the 4.75-mm (No. 4) sieve and larger, and the fine aggregates were defined as the percent of the sample that passed the 4.75-mm (No. 4) sieve.

Binder properties

Binder properties (viscosity and penetration) were also obtained to characterize the samples. Viscosity is defined as the measure of resistance to flow of a fluid. For this evaluation, the kinematic viscosity (ASTM D 2170-01a) of the bitumen was measured at 275°F, which is the approximate temperature for mixing and laydown in hot mix asphalt construction. The testing apparatus was placed in an oil bath, and the time for the known volume of the bitumen to flow through the capillary viscometer was measured. Results typically indicate that the higher the value of viscosity, the harder the binder will be in a solid state. A penetration test (ASTM D 5-06) gives a measure of a bituminous material's stiffness. The penetration of a standard needle is measured vertically at 77°F with a 100-g mass for 5 sec. Results typically indicate that the lower the value of penetration, the stiffer the binder will be in a solid state.

Figure 11 shows the asphalt extraction/recovery process, and Table 3 presents the results for conventional properties of the AC samples.

Figure 11. Obtaining binder properties.

Table 3. AC properties results.

Sample	Viscosity @ 275°F (cS)	Rice Gravity	Percent AC by Extraction	Penetration (0.10 mm)	Coarse Aggregates (%)	Fine Aggregates (%)
VA-3	1370	2.452	4.69	12	36.8	63.2
H-1	1361	2.451	6.0	11	38.2	61.8
H-2	1401	2.525	6.1	14	23.9	76.1
H-3	2820	2.410	5.5	12	22.7	77.3
RG-1	2042	2.581	5.3	8	38.0	62.0
RG-2	790	2.399	6.1	10	29.2	70.8
L-1	9530	2.437	7.0	10	35.5	64.5
L-2	6006	2.495	5.8	12	32.8	67.2
C-1	2162	2.486	4.7	14	34.3	65.7
C-2	810	2.560	4.9	26	38.5	61.5
B-1	700	2.439	5.3	20	31.5	68.5
B-2	497	2.425	6.65	37	40.0	60.0
B-3	18,739	2.451	5.7	4	38.7	61.3
KA-1	15,415	2.499	4.80	3	45.8	54.2
LM	599	2.55	4.90	42	40.5	59.5

Furthermore, dynamic shear rheometer (DSR) tests (ASTM D 7175-05e1) were performed on the extracted binders to characterize the viscous and elastic behavior of binders at high and intermediate service temperatures. The results generally indicate a pavement's resistance to permanent deformation and fatigue cracking. DSR results are commonly summarized as $G^*/(\sin \delta)$ and $G^*(\sin \delta)$ where G^* is the complex shear modulus relating to the total resistance of the binder to shear deformation, and δ is the phase angle relating to the binder's viscous ($\delta=90$) and elastic ($\delta=0$) nature. The term $G^*/(\sin \delta)$ basically characterizes the binder's resistance to rutting. As the value of $G^*/(\sin \delta)$ increases, the tendency of a mix to rut decreases. The term $G^*(\sin \delta)$ provides the binder's resistance to fatigue cracking. As the value of $G^*(\sin \delta)$ increases, the more work will be dissipated per traffic loading cycle (Brown et al. 1996). The aged asphalt binders and the standard laboratory mix binder were evaluated with the DSR test at a temperature of 153°F. The DSR test results are listed in Table 4.

Table 4. DSR test results.

Sample	$G^*/(\sin \delta)$ (MPa)	$G^*(\sin \delta)$ (MPa)
VA-3	0.0616	0.0046
H-1	0.0078	0.0078
H-2	0.0022	0.0021
H-3	0.0464	0.0399
RG-1	0.0882	0.0798
RG-2	0.0315	0.0305
L-1	0.0686	0.0496
L-2	0.0843	0.0582
C-1	0.0395	0.0351
C-2	0.0028	0.0028
B-1	0.0034	0.0034
B-2	0.0015	0.0014
B-3	0.0525	0.0475
KA-1	0.0657	0.3349
LM	0.0014	0.0014

Indirect tensile strength tests

ITS tests (ASTM D 6931-07) are used to determine the tensile strength of AC. For this evaluation, the tests were performed on an Instron machine in the ERDC asphalt laboratory. The Instron machine applies a compressive load at a controlled deformation rate of 2 in. per minute. The loading causes a fairly uniform tensile stress perpendicular to the loading direction, thus yielding a tensile failure. The cored specimens are required to have a 4- or 6-in. nominal diameter and a minimum core height of 1.5 to 2 in. Once the failure load is known, the tensile strength of the cored specimen can be determined using the equation below (ASTM D 6931-07).

$$S_t = \frac{2 * P}{\pi * t * D} \quad (2)$$

S_t = indirect tensile strength, kPa (psi)
P = maximum load, N (lb)
t = cored specimen height, mm (in.)
D = cored specimen diameter, mm (in.)

The ITS tests (Figure 12) were conducted at room temperature on 4-in.-diam cores that were 2.5 in. in height. Approximately three cores were tested per AC sample. Table 5 gives the results of the ITS tests. The results present the average of the three replicates. Peak strength is the maximum compressive load of the sample, and energy to peak strength is measured as the area under the load versus deformation plot.

Fatigue tests

Fatigue life of the aged samples was determined with beam fatigue testing. The apparatus used in this study includes an environmental chamber and performs the Strategic Highway Research Program test procedure (designated M 009). The test can be run either in strain or stress controlled loadings. The AC beams are typically 2.5 in. wide, 2.0 in. tall, and at least 15 in. long. Fatigue is tested in third point loading, and the beams are subjected to repeat flexural bending. Figure 13 shows a picture of the beam fatigue apparatus.

For this evaluation, the tests were run at a constant strain of 550 microstrains, and the environmental chamber was set to a testing temperature of 68°F. The AC beams, 2.5 in. wide, 2.0 in. tall, and 15 in. long, were

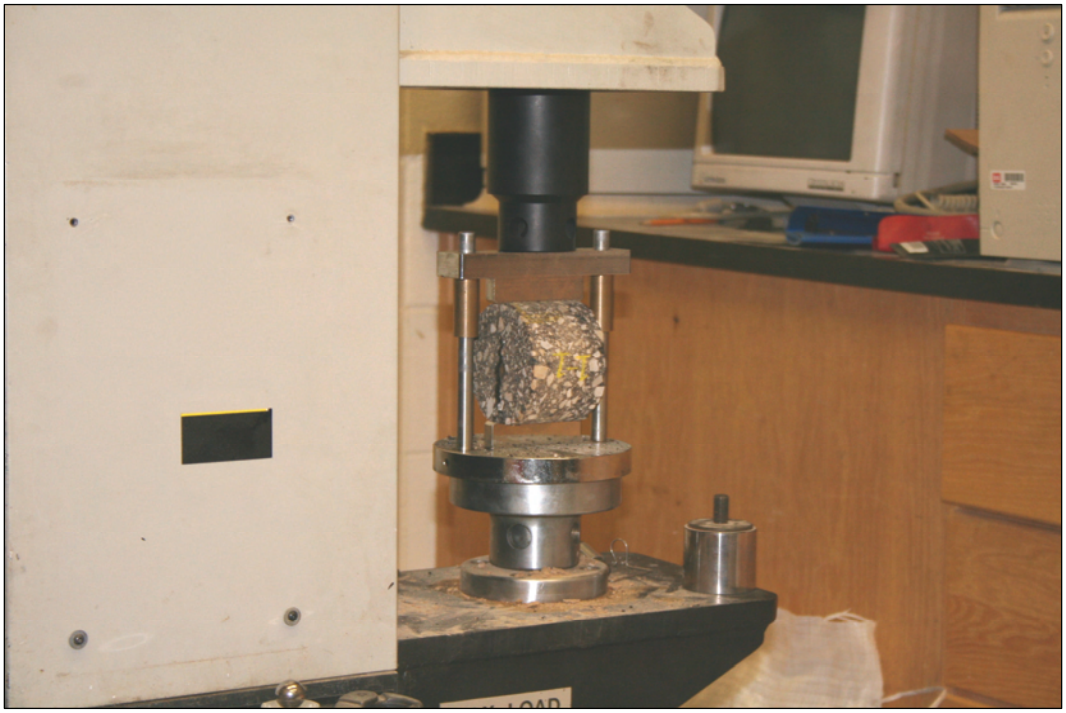

Figure 12. ITS test on the Instron machine.

Table 5. ITS test results.

Sample	Peak Strength (lb)	Compression at Peak Strength (in.)	Energy to Peak Strength (in.-lb)
VA-3	3677	0.0676	124
H-1	3960	0.0727	146
H-2	3817	0.0681	130
H-3	4471	0.0616	138
RG-1	3487	0.0605	110
RG-2	4772	0.0582	139
L-1	1615	0.0541	44
L-2	3467	0.1009	177
C-1	6150	0.0955	293
C-2	5879	0.1029	302
B-1	4184	0.0917	192
B-2	2364	0.0638	75
B-3	2291	0.0590	68
KA-1	3421	0.1031	220
LM	1550	0.1660	129

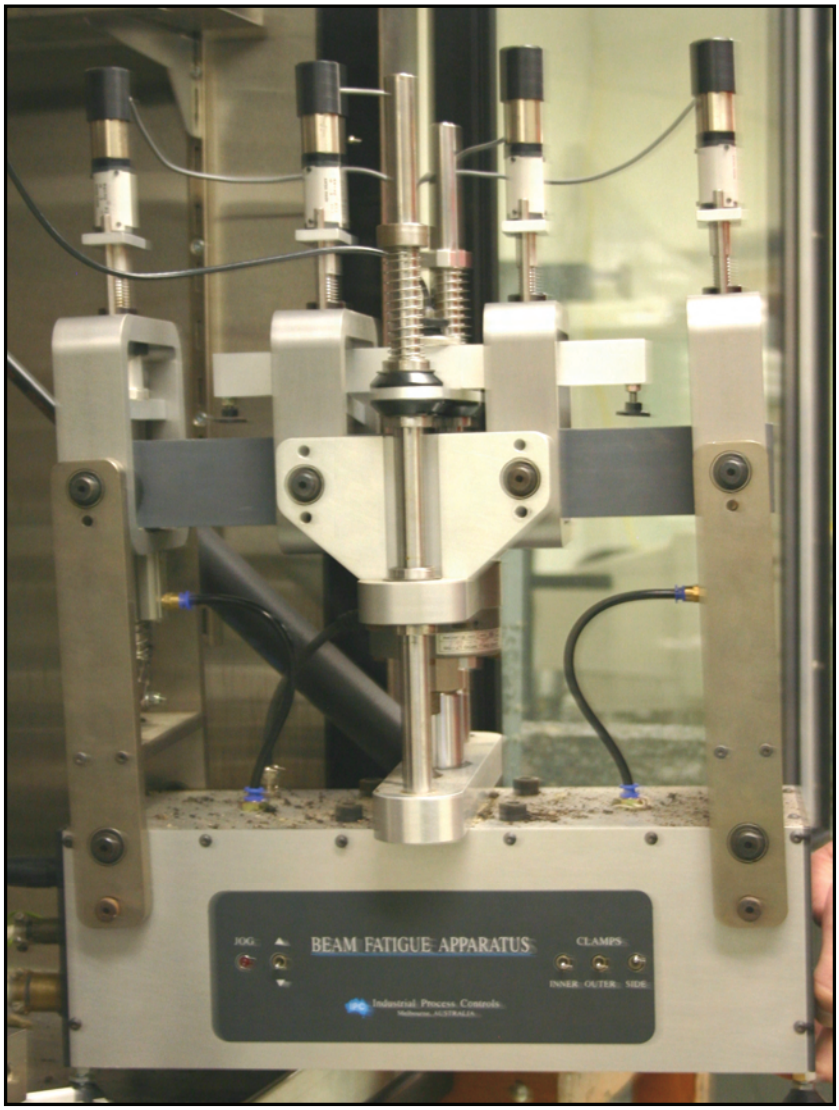

Figure 13. Beam fatigue apparatus.

terminated at 850,000 load cycles (24 hr) or when the stiffness level was at 500 MPa (72,519 psi). Figure 14 shows an example of the beam fatigue results of one of the aged AC samples. Typical beam fatigue results of the aged AC samples show that initially there is internal heating due to strain and friction. Next, there is damage accumulation in the micro-crack formation, and then the micro-cracks coalesce to macro-cracks leading to a breakdown of the sample. Table 6 shows the initial stiffness (50th load cycle) and end cycle of the beam fatigue tests. The end cycle is the number of load repetitions applied before the test was terminated. The results represent the averages of two to four replicates for each sample. The results of the beam fatigue tests will be presented and discussed in detail in the data analysis (Chapter 4).

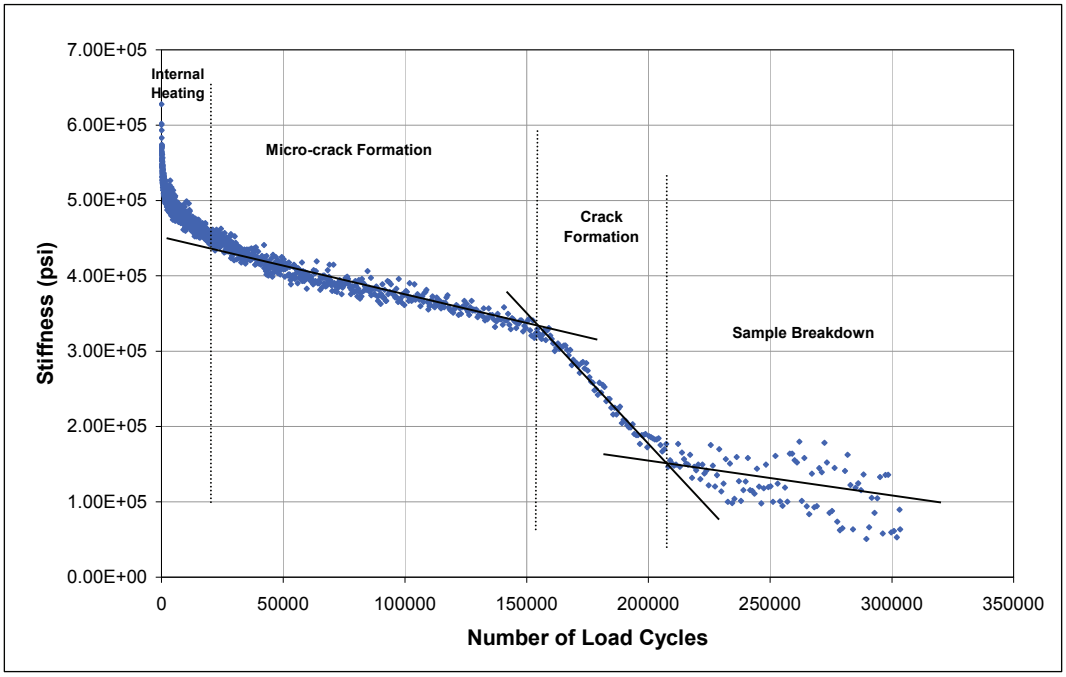

Figure 14. Typical beam fatigue test results for aged AC samples.

Table 6. Beam fatigue test results.

Sample	Initial Stiffness (ksi)	End Cycle
VA-3	743	246,223
H-1	560	677,850
H-2	1290	40,753
H-3	1210	640,415
RG-1	808	92,040
RG-2	1450	313,325
L-1	343	210,965
L-2	804	192,353
C-1	1120	226,893
C-2	1410	132,237
B-1	892	145,580
B-2	518	203,620
B-3	293	366,937
KA-1	151	93,227
LM	466	90,937

Portable seismic pavement analyzer tests

Once the aged AC samples were brought to the ERDC asphalt laboratory, they were placed in a temperature control chamber, and the moduli of the samples were measured at temperatures of 40, 75, and 120°F. The PSPA was placed in exactly the same location on the AC samples at each temperature. The purpose of this procedure was to ensure that the PSPA could pick up the change in temperature of the samples and to determine if the stiffness of an aged AC changes with temperature. Furthermore, the PSPA equation for AC design modulus (Equation 1) was verified by this procedure. Figure 15 shows the outside of the temperature control chamber, and Figure 16 shows the PSPA operating on one of the aged AC samples inside the temperature control chamber. The samples were supported on wooden pedestals during PSPA measurements.

Figure 15. Outside the temperature control chamber.

Figure 17 summarizes the measured PSPA modulus values for the AC pavement samples, where the PSPA was used at three temperatures in the temperature control chamber. Figure 18 shows the same measurements for each individual sample after conversion to design modulus (Equation 1) values. The sample from Kandahar (KA-1) was excluded from this part of the study because it was too large for the temperature control chamber.

Figure 16. Conducting PSPA tests on samples in the temperature control chamber.

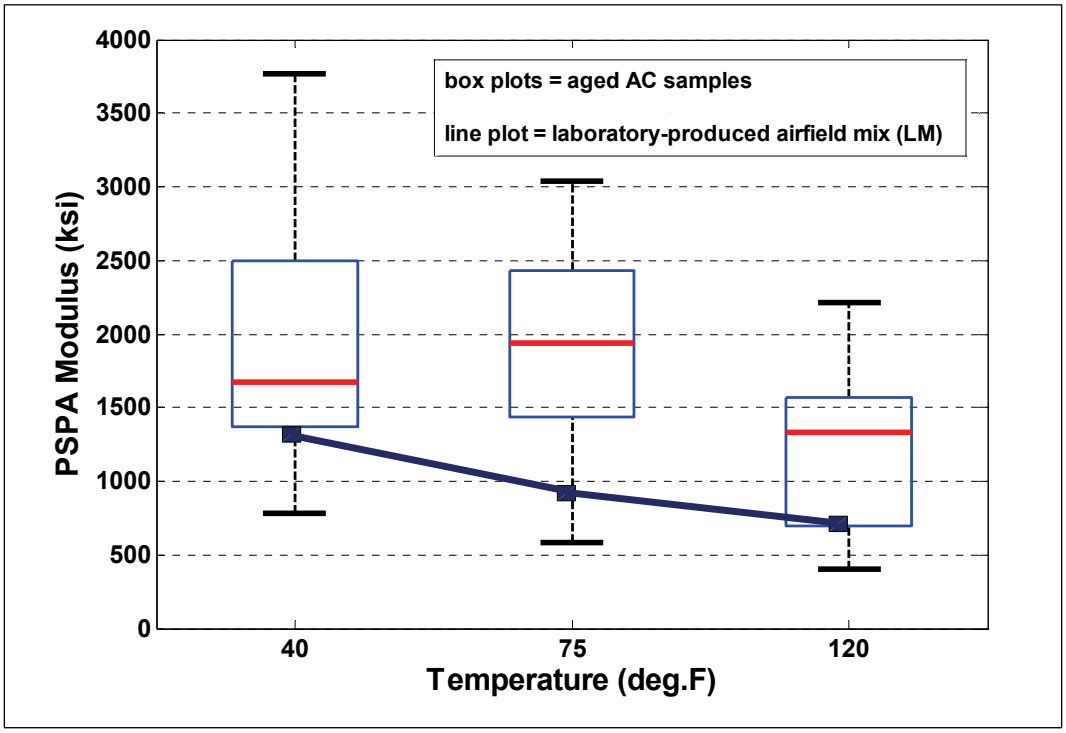

Figure 17. PSPA modulus data from the temperature control chamber.

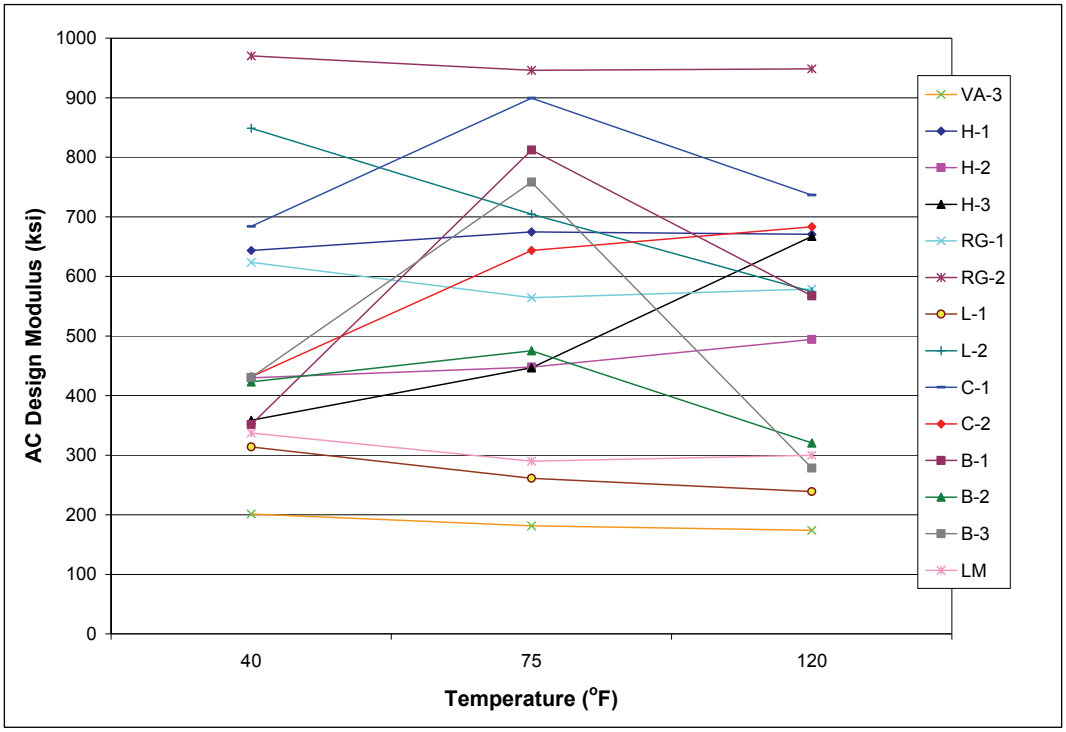

Figure 18. PSPA design modulus data from the temperature control chamber.

In Figure 17, the laboratory-produced AC mixture is presented as a line plot, and the aged AC samples are presented as box plots. In a box plot, the limits of each box represent the range from the 25th percentile to the 75th percentile (i.e., the interquartile range). The horizontal line (red line) within each box is the data median value, and the horizontal lines (black lines) above and below each box represent the extreme values. There were no outliers in these datasets. The laboratory-produced mixture (LM) and the extreme values for the aged AC samples follow the expected trend of decreasing stiffness with increasing temperature. Also, the median value for the aged AC samples at 120°F is lower than the median values for the two lower temperatures. However, the interquartile ranges for the 40°F data and the 75°F data are similar. This can be attributed to one of two causes:

a. The PSPA had difficulty with the measurements on the small wooden slabs.

b. The PSPA was accurate in identifying that the difference in high-frequency moduli between 40 and 75°F is small for aged AC pavements.

Difficulties in obtaining reliable PSPA measurements could have been due to edge effects (i.e., the finite horizontal slab dimensions), the absence of continuous support under the AC, and/or difficulties in effective contacts between the PSPA and the surface of the slabs. The negligible difference between PSPA moduli at 40 and 75°F is attributed to the high stiffness values measured at room temperature (75°F) relative to the laboratory-produced mixture (LM). The high stiffness values of the aged AC samples at room temperature are a consequence of the asphalt aging process.

The AC design modulus equation (Equation 1) is used for the purpose of

a. negating the influence of different testing temperatures

b. normalizing data to a single loading frequency of 15 Hz (Nazarian et al. 2005).

Therefore, the expected trend for Figure 18 is for the AC design moduli to be relatively the same at each temperature. Overall, the averages and the ranges of data for the three temperatures are similar. Also, the approximate average of AC design moduli (600 to 700 ksi) and the range of AC design moduli (200 to 1000 ksi) are reasonable according to information published by Yoder and Witczak (1975) and Huang (1993). These authors reported that the expected average and range for AC modulus (at 16-Hz loading and 70°F) was 700 ksi and 500 to 1100 ksi, respectively.

However, Figure 18 also shows some individual pavement samples that exhibited substantial changes between moduli at different temperatures (H-3, C-1, C-2, B-1, B-2, and B-3). Again, these odd data could be attributed to the PSPA device having difficulty either with finite slabs or with achieving effective contact on the rough AC surfaces.

Based on these limited data, the AC design modulus equation (Equation 1) appears to be reasonable. However, when using the PSPA to obtain data for airfield pavement evaluations, many measurements (10 or more) should be collected for each airfield feature. The large number of replicates will serve as a precaution to counteract the possibility for poor data as caused by poor contact between the PSPA and the AC pavement.

4 Data Analysis

Introduction

This chapter is dedicated to analyzing the results presented in the previous chapter, as well as elaborating on beam fatigue results. Specifically, the fatigue data will be used to develop an adjustment to current pavement design criteria to be used for the purpose of evaluating pavements with aged AC surfaces.

Current Department of Defense criterion

The current DoD criterion for fatigue of AC pavements is in terms of allowable strain repetitions, ε_r (Headquarters, Departments of the Army, the Navy, and the Air Force 2001b):

$$\varepsilon_r = 10^x \tag{3}$$

X = 2.68-5.0*Log S_A -2.665*Log E

S_A = tensile strain of AC, in./in.
E = elastic modulus of AC, psi

Equation 3 was derived from a graphical plot of allowable load repetitions, in terms of both strain and stress (Figure 19), which was proposed by Barker and Brabston (1975) for use by the U.S. Army Corps of Engineers. The plot was originally presented in the United States by Heukelom and Klomp (1963), who referenced Nijboer (1959) as the original developer.

Defining failure for beam fatigue tests

When picking a type of beam fatigue test, constant stress tests are generally considered to provide reasonable representation for relatively thick (>6 in.) AC surface layers on pavements. Constant strain tests are considered to provide reasonable representation for relatively thin (<2 in.) AC surface layers on pavements. AC surface layers with thicknesses intermediate to these limits will show fatigue responses that are between these two modes (Yoder and Witczak 1975).

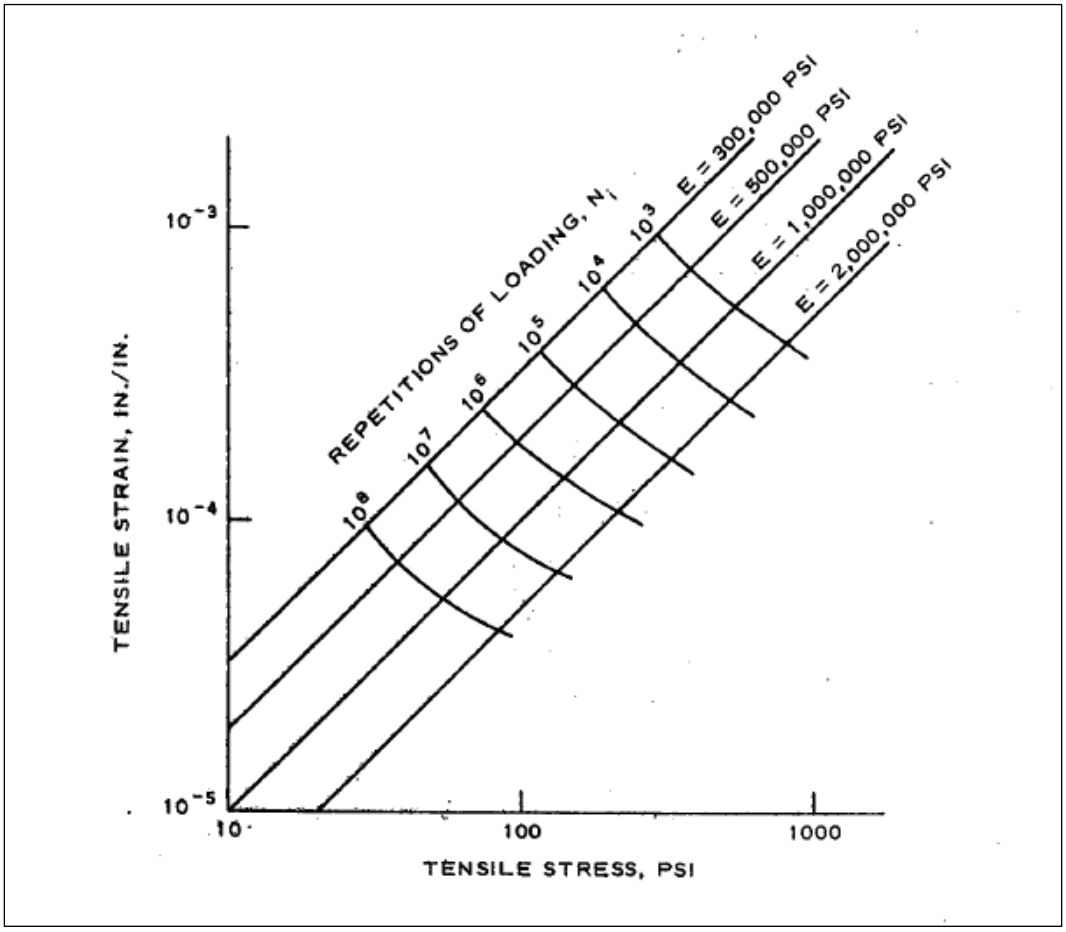

Figure 19. Fatigue data for bituminous concrete materials (after Nijboer 1959).

An advantage of constant stress tests (not used in this study) is that the failure of beams is relatively easy to define. As a beam is damaged in these tests, modulus decreases and larger deflections are required to produce the same target stress. With stress levels that are reasonable for pavements, the beams will eventually break.

An advantage of the constant strain test, such as that used in this study, is that predictions of strain in a simply supported beam do not require any estimate for AC modulus; strain can be controlled via the measured deflection at the bottom of the beam. Unfortunately, the failure of beams tested in this manner is not easy to define. As a beam is damaged in these tests, modulus decreases, and the same imposed deflections produce progressively smaller stresses. With strain levels that are reasonable for pavements, the beams will not break. As a consequence, arbitrary definitions for beam failure have been established, such as the number of repetitions at the time that beam stiffness is reduced to 50% of its initial value (Yoder and Witczak 1975). Beam stiffness reductions from 40 to 80% have been

explored for the purpose of defining beam failure (Kingham and Kallas 1972). Typically, initial stiffness in a beam test is defined as that attained after some quantity of "conditioning" repetitions; 200 repetitions is common for this purpose (Kingham and Kallas 1972, Yoder and Witczak 1975).

This study offered a unique combination of fatigue test results. While tests are typically conducted only on laboratory-produced beams, this study included a combination of both laboratory-produced beams and beams sawn from field samples. This broad range of beam sources led to a broad range of beam test results, which then led to the need for a reexamination of how beam test results are quantified.

While defining the "initial stiffness" for beams as the stiffness at 200 repetitions appears to be reasonable for laboratory-produced samples (Figure 20), this definition would exclude useful information for some of the aged AC samples (Figure 21). One of the field samples from Butts Army Airfield (Figure 21) lost about 1/3 of its stiffness within the first 200 repetitions. For the purposes of this study, initial stiffness was defined as the earliest stiffness value where the fatigue plot (Figures 20 and 21) retained a smooth concave up or concave down shape. For the laboratory mixture (Figure 20), this stiffness value nearly matched the stiffness at 200 replicates. For the field sample (Figure 21), this stiffness value was higher than the stiffness at 200 replicates.

Rather than defining the "repetitions at beam failure" as some arbitrary percentage of lost stiffness, a definition for beam failure was derived using the current DoD asphalt strain criterion and the laboratory-produced standard airfield mixture. The PSPA modulus for the standard airfield mixture was applied to the current DoD criterion, along with the knowledge that the beams were tested at 550 microstrains, to determine the predicted cycles to failure. Given a PSPA modulus of 452 ksi (corrected to 77°F), the predicted cycles at failure was 8,080. Findings for the three replicate beams of standard airfield mixtures are shown in Figures 22 through 24, and they are summarized in Table 7. The average percent stiffness at predicted failure for these mixtures was approximately 73%. Therefore, "failure" for all beam tests conducted in this study was defined as the number of fatigue cycles required to reduce beam stiffness to 73% of its initial value. Average cycles to failure are summarized for all samples in Table 8.

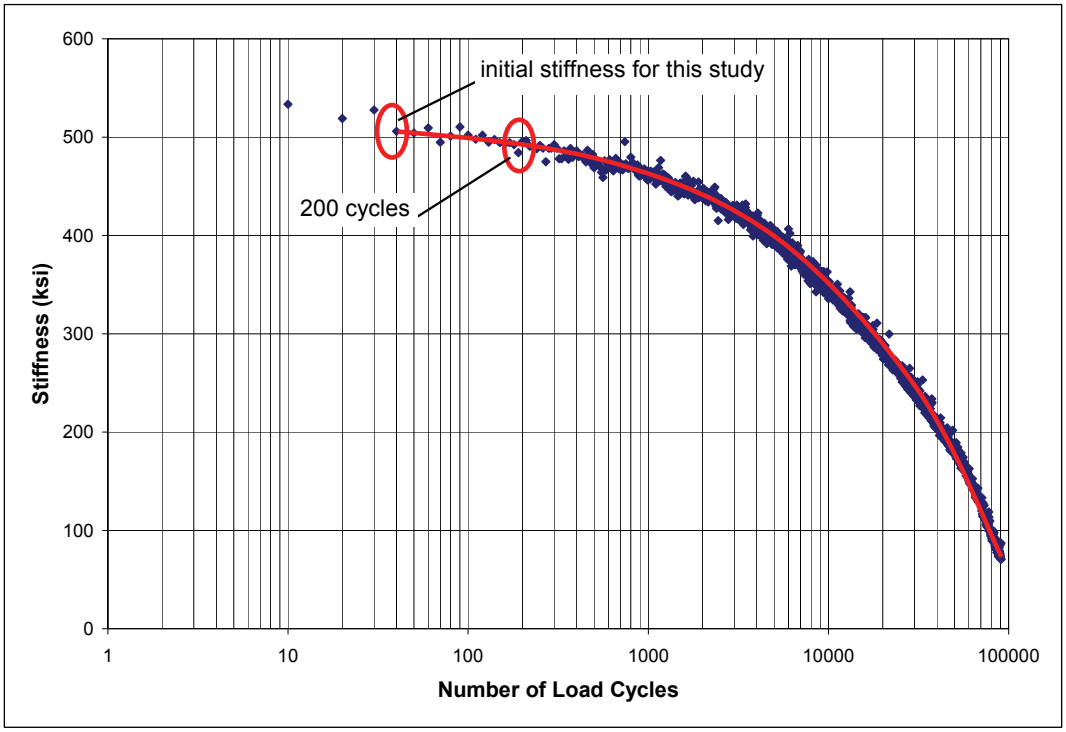

Figure 20. Laboratory-produced standard airfield mixture (LM), replicate 3.

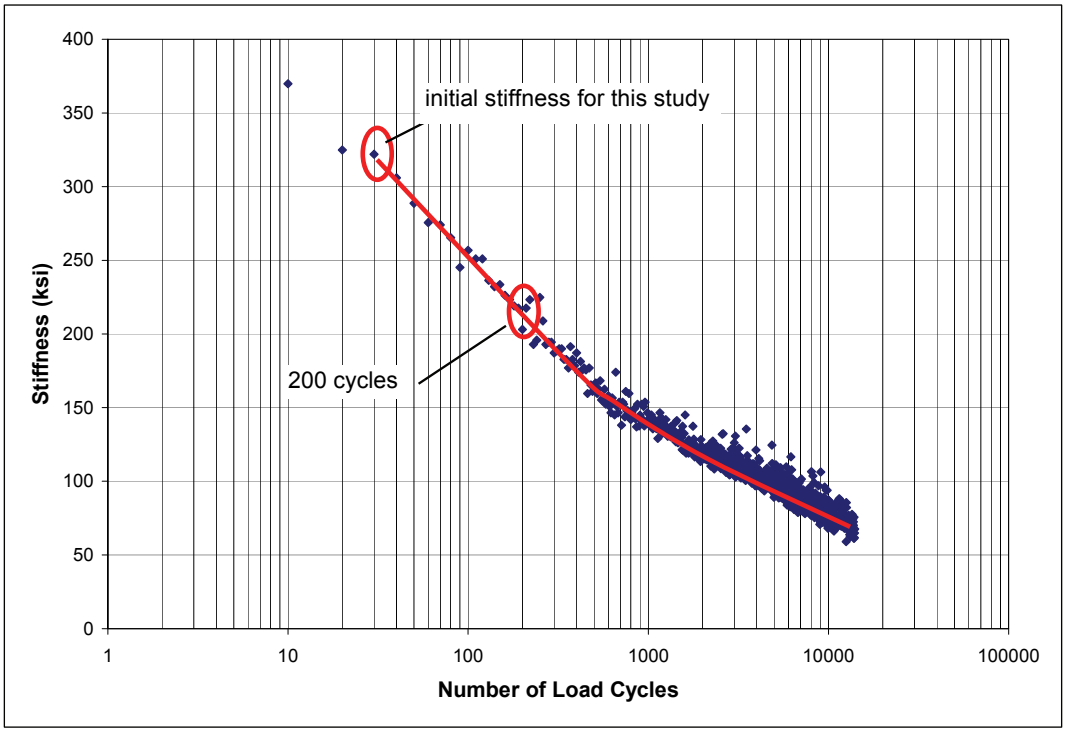

Figure 21. Butts Army Airfield field sample (B-2), replicate 2.

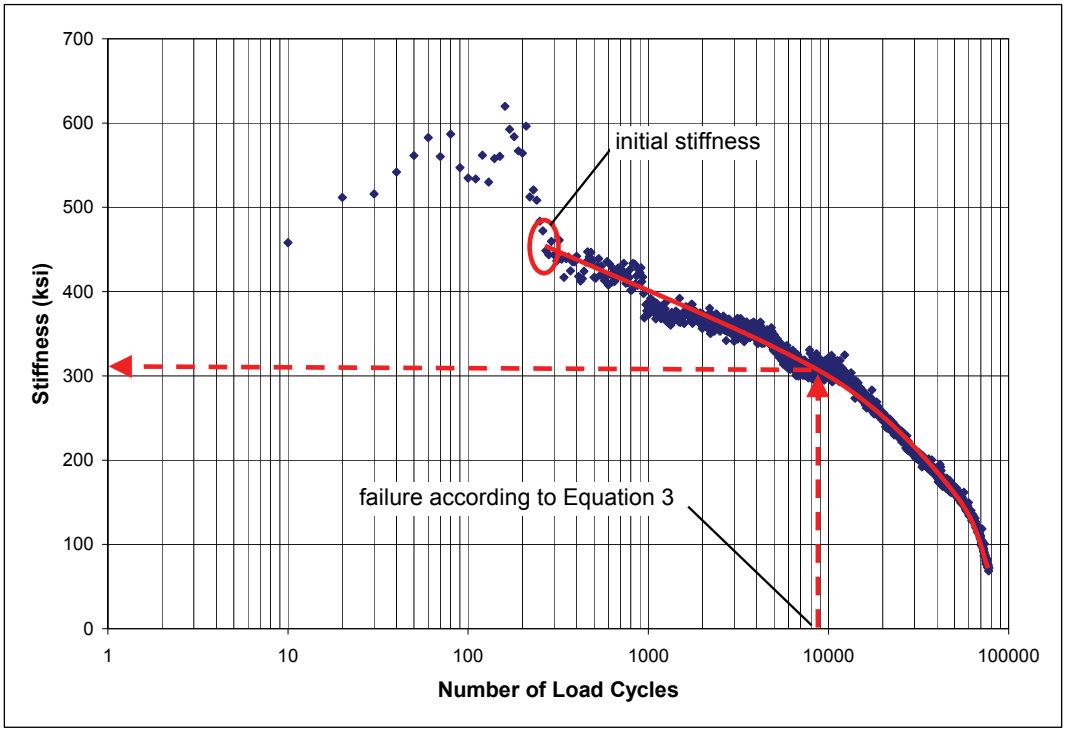

Figure 22. Establishing percent stiffness at failure for the laboratory-produced standard airfield mixture (LM), replicate 1.

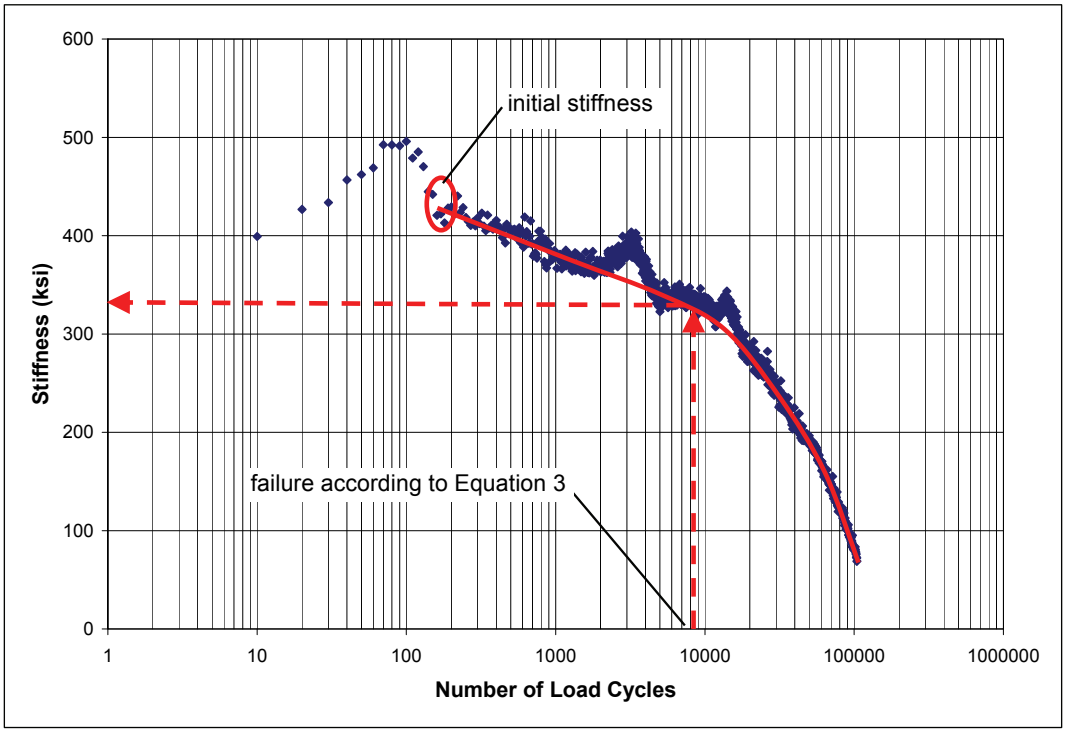

Figure 23. Establishing percent stiffness at failure for the laboratory-produced standard airfield mixture (LM), replicate 2.

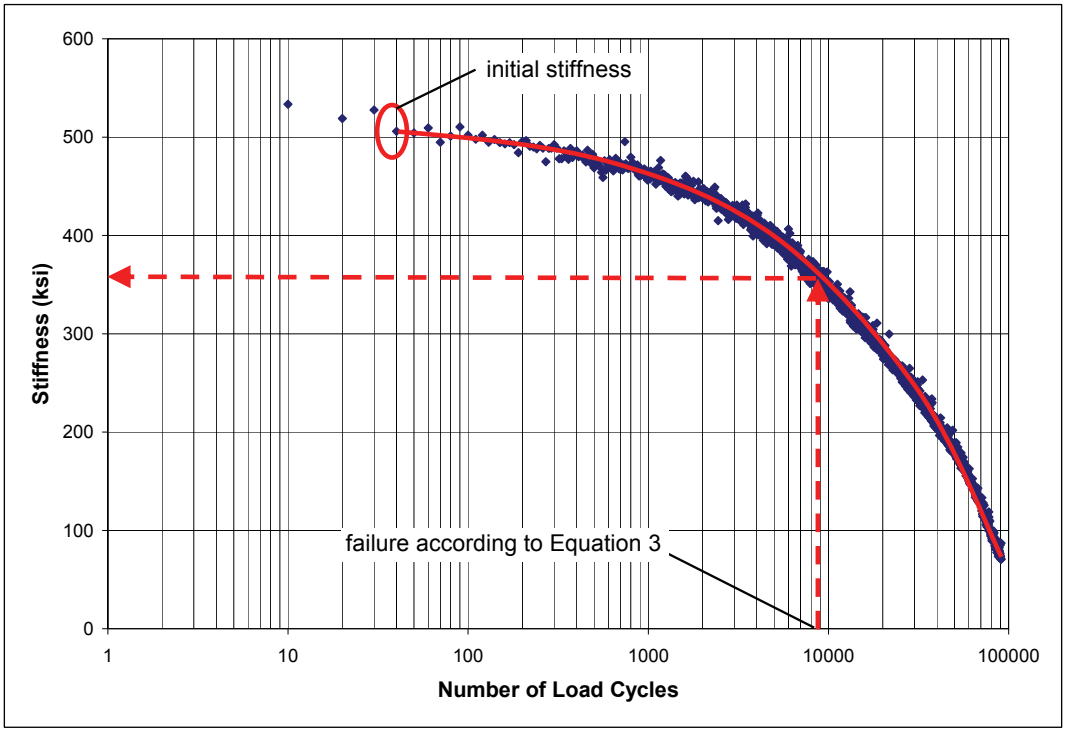

Figure 24. Establishing percent stiffness at failure for the laboratory-produced standard airfield mixture (LM), replicate 3.

Table 7. Summary of fatigue results for laboratory-produced standard airfield mixture (LM).

Replicate	Cycles at Initial Stiffness	Initial Beam Stiffness (ksi)	Predicted Cycles to Fatigue Failure[a]	Stiffness at Predicted Failure (ksi)	Percent of Initial Beam Stiffness at Failure
1	270	449	8,080	310	69
2	150	442	8,080	339	77
3	40	506	8,080	365	72

[a] Determined using Equation 3; 550 microstrains and PSPA modulus = 452 ksi (corrected to 77 °F).

Beam fatigue results versus current DoD criterion

To quantify the ability for the current DoD criterion to predict fatigue failure in aged AC, the criterion was used to predict cycles to failure for each of the samples under conditions matching the beam fatigue tests (i.e., 550 microstrains). Again, the PSPA data were used to estimate modulus at room temperature, which was the condition for the fatigue tests. Basic comparisons of measured cycles to failure versus predicted cycles to failure are shown in Figure 25. While the laboratory-produced standard

Table 8. Average cycles to failure for all sample types.

Sample	Cycles at Initial Stiffness	Initial Beam Stiffness (ksi)	Average Cycles to Failure[a]
VA-3	30	743	593
H-1	73	560	3,260
H-2	58	1290	9,280
H-3	50	1210	937
RG-1	40	808	1,310
RG-2	30	1450	4,720
L-1	40	343	1,240
L-2	53	804	4,040
C-1	48	1120	6,330
C-2	47	1410	4,420
B-1	58	892	7,390
B-2	43	518	5,980
B-3	70	293	1,200
KA-1	50	151	3,800
LM	153	466	8,330

[a] Failure is defined as the number of cycles when stiffness drops to 73% of its initial value. Average is obtained from replicate values of LOG_{10} (cycles).
Note: Results represent averages of two to four replicates.

airfield mixture (LM) falls on the line of equality, the field samples are scattered over both the conservative and unconservative regions of the plot. The correlation coefficient between Log_{10} (predicted cycles) and Log_{10} (measured cycles) to failure for the aged AC samples was -0.27 (essentially zero). As the worst case of a conservative prediction, the measured cycles to failure were higher than the value predicted by a factor of six. As the worst case of an unconservative prediction, the measured cycles to failure were lower than the value predicted by a factor of 30.

To facilitate further analyses and refinement of the current DoD criterion, the level of conservatism needed to be represented as a single value. This was accomplished using the base 10 Log of the ratio of cycles as follows:

$$Log\ Ratio = Log_{10}\left(\frac{\text{measured cycles}}{\text{predicted cycles}}\right) \quad (4)$$

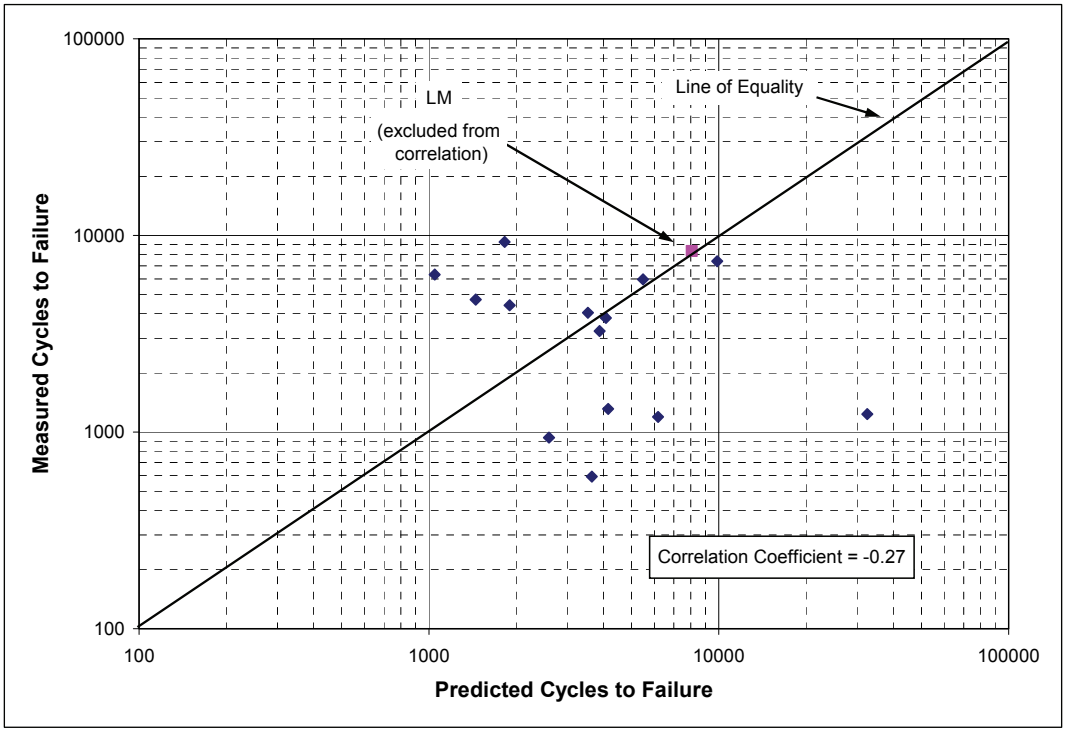

Figure 25. Comparison of predicted and measured cycles to beam fatigue failure.

measured cycles = cycles to failure in the beam fatigue test (73% of initial stiffness)
predicted cycles = cycles to failure using current DoD criteria (Equation 3)

Given that fatigue data often involve several orders of magnitude in range, the use of logarithms kept the data within limits that were easy to plot and compare. Also, logarithms tend to normalize fatigue data that typically have positive skew. While using Log Ratio as defined in Equation 4, the following rules apply to calculated quantities:

a. If Log Ratio = +2, the measured cycles to failure exceeded the predicted cycles to failure by a factor of 100.

b. If Log Ratio = +1, the measured cycles to failure exceeded the predicted cycles to failure by a factor of 10.

c. If Log Ratio = 0, the measured cycles to failure equaled the predicted cycles to failure.

d. If Log Ratio = -1, the predicted cycles to failure exceeded the measured cycles to failure by a factor of 10.

e. If Log Ratio = -2, the predicted cycles to failure exceeded the measured cycles to failure by a factor of 100.

In summary, positive numbers represent conservative predictions by the current DoD criterion, and negative numbers represent unconservative predictions by current DoD criterion. Table 9 shows predicted cycles to failure, measured cycles to failure, and the average Log Ratio for each mixture. The failure prediction for the standard airfield laboratory mixture (LM) closely matches the measured cycles to failure because the definition for beam fatigue failure was derived using these laboratory-produced samples in comparison to the current DoD criterion (Equation 3). The Log Ratio of the aged field samples ranges from -1.42 to +0.78. It is again

Table 9. Comparisons of predicted versus measured cycles to failure.

Sample	Predicted Cycles to Failure[a]	Measured Cycles to Failure[b]	Log Ratio[c]
VA-3	3,650	593	-0.79
H-1	3,880	3,260	-0.08
H-2	1,820	9,280	0.71
H-3	2,600	937	-0.44
RG-1	4,160	1,310	-0.50
RG-2	1,450	4,720	0.51
L-1	32,500	1,240	-1.42
L-2	3,540	4,040	0.06
C-1	1,050	6,330	0.78
C-2	1,900	4,420	0.37
B-1	9,890	7,390	-0.13
B-2	5,480	5,980	0.04
B-3	6,170	1,200	-0.71
KA-1	4,080	3,800	-0.03
LM	8,080	8,330	0.01

[a] Predicted using current DoD criterion (Equation 3) with 550 microstrains and the PSPA modulus corrected to 77°F.

[b] Measured using 73% of the initial stiffness from the beam fatigue data.

[c] As defined by Equation 4.

apparent that the current DoD criterion has difficulty predicting failure for aged AC samples obtained from the field, with predictions ranging from overly conservative to unconservative. The next section in this report will investigate methods for using additional physical and mechanical characteristics of the AC to improve predictions relating to fatigue behavior.

Predicting current DoD criterion inaccuracies (Log Ratio) for aged AC

This analysis was performed to determine whether additional AC characteristics could be used to predict the Log Ratio, as presented in the preceding section. This prediction will be necessary for improving the current DoD fatigue criterion for aged AC. The additional asphalt characteristics are summarized in Tables 10 through 13, which categorize the data according to

a. field parameters

b. ITS parameters

c. AC mixture parameters

d. asphalt binder parameters.

These categories are listed in order from the easiest parameters to measure to the most difficult parameters to obtain. In other words, a pavement evaluation team could obtain the field parameters relatively easily. In contrast, obtaining asphalt samples for the purpose of characterizing mixture proportions or binder properties would be time-consuming. The analysis was conducted in five stages, with each stage representing the use of a different set of parameters for the purpose of improving predictions of fatigue behavior. The first four stages reflected the same groupings as Tables 10 through 13, and the fifth stage combined all available data. The analysis for each stage assumed that all data within the relevant group or groups would be available as independent variables; the dependent variable was Log Ratio. The analysis for each stage was performed with a multivariate linear regression, which was accomplished with the STEPWISE tool within MATLAB® software. This procedure is essentially a forward-selection procedure for stepwise regression in which statistically significant independent variables are added to the predictive regression equation in an order that starts with the most significant variable. The laboratory-produced standard airfield mixture (LM) was not included in these

Table 10. Field parameters.

Sample	Log Ratio	Pavement Surface Age (yr)	PSPA Modulus (ksi)
VA-3	-0.79	41	609
H-1	-0.08	25	595
H-2	0.71	19	790
H-3	-0.44	35	692
RG-1	-0.50	19	580
RG-2	0.51	55	861
L-1	-1.42	27	268
L-2	0.06	27	616
C-1	0.78	12	973
C-2	0.37	50	778
B-1	-0.13	5	419
B-2	0.04	42	523
B-3	-0.71	42	500
KA-1	-0.03	30	584
LM[a]	0.01	0	452
[a] Excluded from multivariate analyses.			

analyses because the analyses were directed toward aged field samples. The possibility of combining parameters from different groups will be discussed after analyzing each group of parameters separately.

The regression using field parameters found the PSPA modulus to be the only significant independent variable (Table 14). Significance is judged by P-value, which is the probability of being incorrect if the independent variable is identified as contributing significantly to the prediction of the dependent variable. P-values shown represent those at the end of the stepwise procedure. Generally, independent variables with P-values less than 0.05 (5%) are considered to be worthy of including in the regression model. The resulting predictive equation is shown as a footnote in the table, along with RMSE, R^2, and adjusted R^2. The RMSE is the root mean squared error (often called the standard error of estimate), which represents the average absolute deviation between actual data and predictions based on the regression (Younger 1979). The R^2 is the coefficient of determination, which provides a measure of the amount of response variability explained by the model. Although the R^2 provides a measure of "goodness

Table 11. ITS test parameters.

Sample	Log Ratio	Peak Strength (kips)	Compression at Peak Strength (mils)	Area Under Curve to Peak (in.-lb)
VA-3	-0.79	3.68	68	124
H-1	-0.08	3.96	73	146
H-2	0.71	3.82	68	130
H-3	-0.44	4.47	62	138
RG-1	-0.50	3.49	60	110
RG-2	0.51	4.77	58	139
L-1	-1.42	1.62	54	44
L-2	0.06	3.47	101	177
C-1	0.78	6.15	95	293
C-2	0.37	5.88	103	302
B-1	-0.13	4.18	92	192
B-2	0.04	2.36	64	75
B-3	-0.71	2.29	59	68
KA-1	-0.03	3.42	103	220
LM[a]	0.01	1.17	173	99

[a] Excluded from multivariate analyses.

of fit," comparisons of R^2 between different regression models that contain different quantities of either independent variables or data points are inaccurate because R^2 is affected by these quantities as well as the steepness of the regression equation slope. To facilitate comparisons between models with different quantities of either independent variables or data points, the adjusted R^2 has been defined as follows (Seber 1977).

$$adjusted\ R^2 = 1 - \left(1 - R^2\right) * \left(\frac{n}{n-p}\right) \tag{5}$$

R^2 = coefficient of determination
n = number of data points
p = number of independent variables plus model intercept

The regression using ITS parameters found the peak strength to be the only significant independent variable (Table 15).

Table 12. AC mixture parameters.

Sample	Log Ratio	Rice Gravity	Percent Binder	Percent Coarse Aggregate
VA-3	-0.79	2.452	4.7	36.8
H-1	-0.08	2.451	6.0	38.2
H-2	0.71	2.525	6.1	23.9
H-3	-0.44	2.410	5.5	22.7
RG-1	-0.50	2.581	5.3	38.0
RG-2	0.51	2.399	6.1	29.2
L-1	-1.42	2.437	7.0	35.5
L-2	0.06	2.495	5.8	32.8
C-1	0.78	2.486	4.7	34.3
C-2	0.37	2.560	4.9	38.5
B-1	-0.13	2.439	5.3	31.5
B-2	0.04	2.425	6.7	40.0
B-3	-0.71	2.451	5.7	38.7
KA-1	-0.03	2.499	4.8	45.8
LM[a]	0.01	2.550	4.9	40.5
[a] Excluded from multivariate analyses.				

The regression using AC mixture parameters found that none of the independent variables provided a significant contribution to explaining the variability of Log Ratio (Table 16).

Similarly, the regression using asphalt binder parameters found that none of the independent variables provided a significant contribution to explaining the variability of Log Ratio (Table 17).

To investigate the potential benefit by combining groups of asphalt characteristics, a multivariate linear regression was conducted with all data together. The ability to predict Log Ratio was found to be improved by combining PSPA modulus and G*/(sin δ) data (Table 18). In this analysis, ITS peak strength dropped out as a significant contributor. Even a separate analysis with PSPA modulus and ITS peak strength alone found ITS peak strength as not improving the regression. The reason ITS peak strength did not help with the combined regression is that this parameter was well correlated with PSPA modulus (Figure 26). Therefore, PSPA modulus already explained the information that could be contributed by

Table 13. Asphalt binder parameters.

Sample	Log Ratio	Penetration (0.10 mm)	Viscosity at 275°F (cS)	G*/(sin δ) (MPa)	G*(sin δ) (MPa)
VA-3	-0.79	12	1370	0.0616	0.0046
H-1	-0.08	11	1360	0.0078	0.0078
H-2	0.71	14	1400	0.0022	0.0021
H-3	-0.44	12	2820	0.0464	0.0399
RG-1	-0.50	8	2040	0.0882	0.0798
RG-2	0.51	10	790	0.0315	0.0305
L-1	-1.42	10	9530	0.0686	0.0496
L-2	0.06	12	6010	0.0843	0.0582
C-1	0.78	14	2160	0.0395	0.0351
C-2	0.37	26	810	0.0028	0.0028
B-1	-0.13	20	700	0.0034	0.0034
B-2	0.04	37	500	0.0015	0.0014
B-3	-0.71	4	18700	0.0525	0.0475
KA-1	-0.03	3	15400	0.0657	0.3349
LM[a]	0.01	42	600	0.0014	0.0014
[a] Excluded from multivariate analyses.					

Table 14. Multivariate linear regression for field parameters.

Independent Variable	P-value
Pavement Surface Age (yr)	0.2915
PSPA Modulus (ksi)	0.0003[a]
[a] Statistically significant (P-value ≤ 0.05) Log Ratio = -1.8532 + 0.002767 * (PSPA modulus, ksi) RMSE = 0.3680, R^2 = 0.67, adjusted R^2 = 0.62	

Table 15. Multivariate linear regression for ITS test parameters.

Independent Variable	P-value
Peak Strength (kips)	0.0049[a]
Compression at Peak Strength (mils)	0.5275
Area Under Curve to Peak (in.-lb)	0.6919
[a] Statistically significant (P-value ≤ 0.05) Log Ratio = -1.4267 + 0.3425 * (ITS peak strength, kips) RMSE = 0.4554, R^2 = 0.50, adjusted R^2 = 0.41	

Table 16. Multivariate linear regression for AC mixture parameters.

Independent Variable	P-value
Rice Gravity	0.4232
Percent Binder	0.4077
Percent Coarse Aggregate	0.4340

Table 17. Multivariate linear regression for asphalt binder parameters.

Independent Variable	P-value
Penetration (0.10 mm)	0.3068
Viscosity at 275°F (cS)	0.1379
G*/(sin δ) (MPa)	0.0589
G*(sin δ) (MPa)	0.8197

Table 18. Multivariate linear regression using all asphalt characteristics.

Independent Variable	P–value
Pavement Surface Age (yrs)	0.1988
PSPA Modulus (ksi)	0.0003[a]
ITS Peak Strength (kips)	0.8112
ITS Compression at Peak Strength (mils)	0.0543
ITS Area Under Curve to Peak (in.-lb)	0.3079
Rice Gravity	0.3196
Percent Binder	0.8378
Percent Coarse Aggregate	0.5576
Penetration (0.10 mm)	0.7075
Viscosity at 275°F (cS)	0.7549
G*/(sin δ) (MPa)	0.0325[a]
G*(sin δ) (MPa)	0.1603
[a] Statistically significant (P-value ≤ 0.05) Log Ratio = -1.4178 + 0.002501 * (PSPA Modulus, ksi) – 6.7663 * (G*/(sin δ), MPa) RMSE = 0.3093, R^2 = 0.79, adjusted R^2 = 0.73	

ITS peak strength. In contrast, G*/(sin δ) showed no correlation to PSPA modulus (Figure 27). Therefore, the binder properties, as exposed by G*/(sin δ), provided information that was different from and complementary to the information provided by the PSPA modulus.

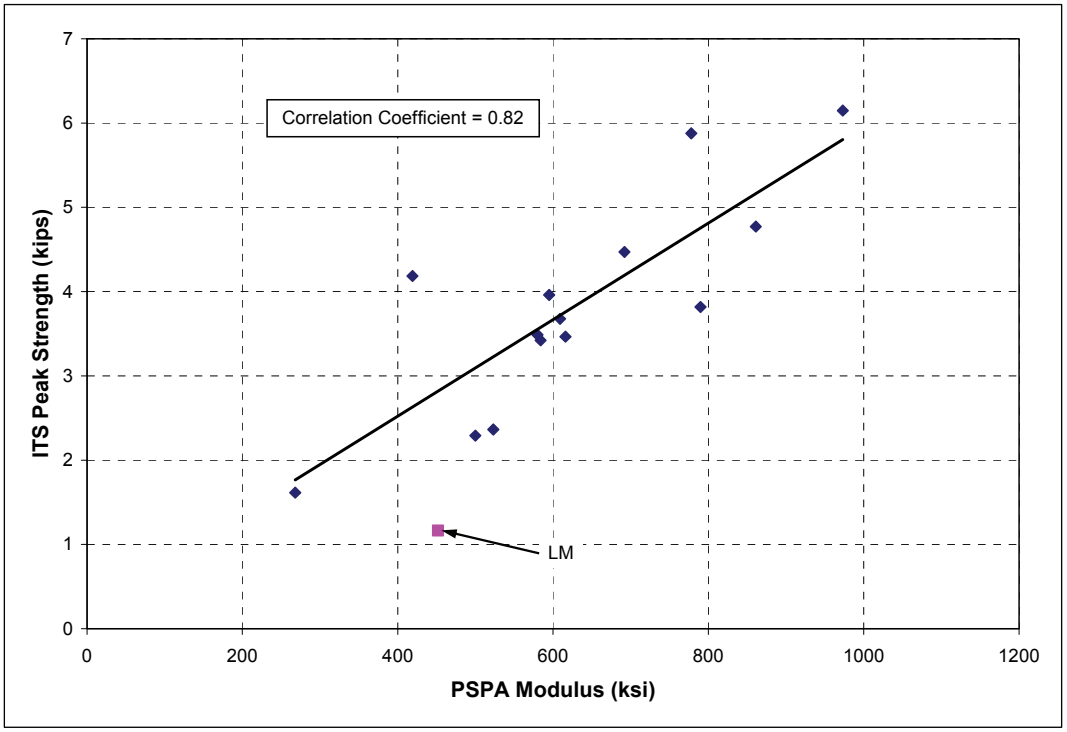

Figure 26. Relationship between PSPA modulus and ITS peak strength.

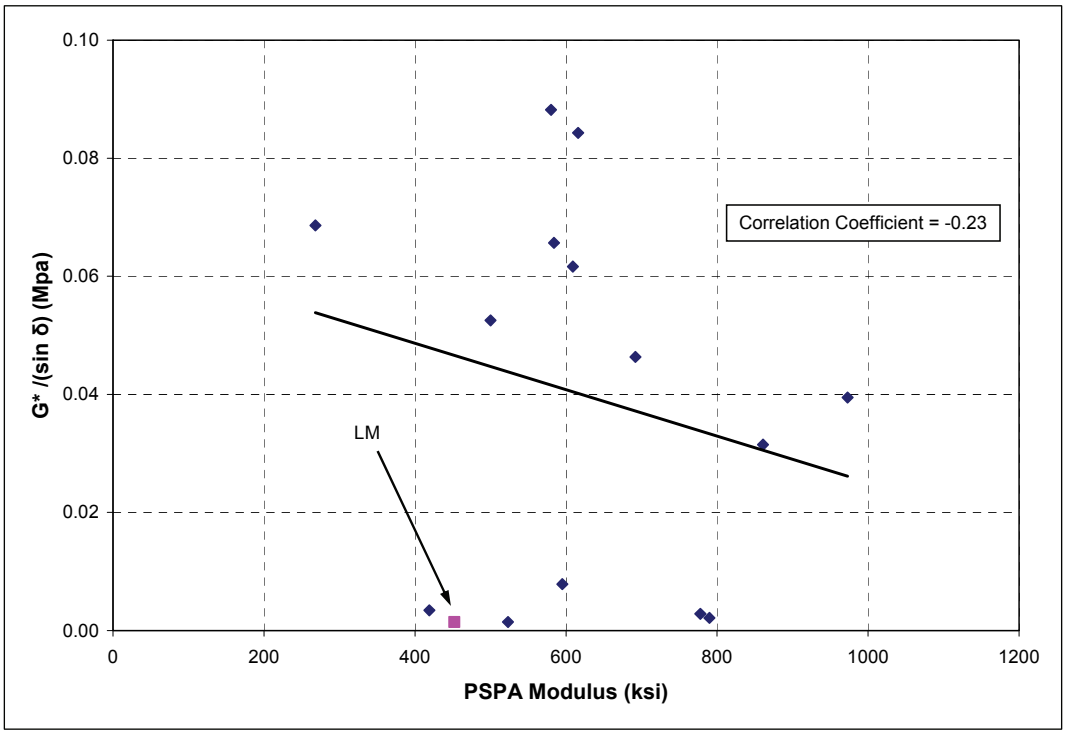

Figure 27. Relationship between PSPA modulus and G*/(sin δ).

In summary, several asphalt characteristics were investigated as part of an effort to predict the Log Ratio, that is, the error in the current DoD fatigue criterion as it relates to aged AC. The best single asphalt characteristic for this purpose was found to be the PSPA modulus, which can be measured in the field. In this case, the prediction for Log Ratio would be (Figure 28):

$$Log\ Ratio = -1.8532 + 0.002767 * (PSPA\ modulus, ksi) \quad (6)$$

$$R^2 = 0.67$$

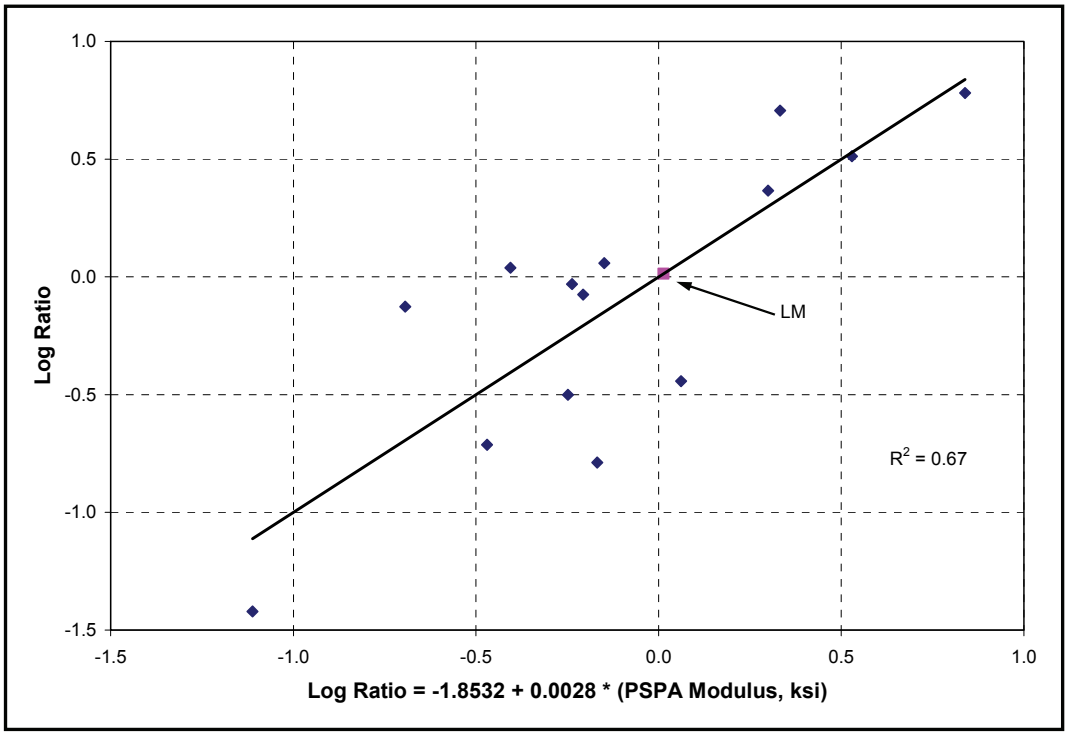

Figure 28. Prediction of Log Ratio using PSPA modulus.

The only other asphalt characteristic that offered significant predictive capability for Log Ratio was ITS, as shown in Figure 29. This test would require obtaining 4-in.-diam cores from the pavement.

$$Log\ Ratio = -1.4267 + 0.3425 * (ITS\ peak\ strength, kips) \quad (7)$$

$$R^2 = 0.50$$

Overall, the most preferred method for predicting Log Ratio would be to use a combination of PSPA modulus and G*/(sin δ) (Figure 30).

$$Log\ Ratio = -1.4178 + 0.0025 * (PSPA\ modulus, ksi) - 6.7663 * (G^* / (\sin\delta), MPA) \quad (8)$$

$$R^2 = 0.79$$

Improved DoD criteria for predicting fatigue behavior of aged AC

The regression equations were next used to adjust the current DoD fatigue criterion. The adjusted fatigue criterion would provide improved accuracy for aged AC pavements. Again, based on the data set included in this study, aged AC pavements would include those 10 years old or older.

Recall the definition for Log Ratio:

$$Log\ Ratio = Log_{10}\left(\frac{\text{measured cycles}}{\text{predicted cycles}}\right) \quad (4)$$

measured cycles = cycles to failure in the beam fatigue test (73% of initial stiffness)

predicted cycles = cycles to failure using current DoD criteria (Equation 3)

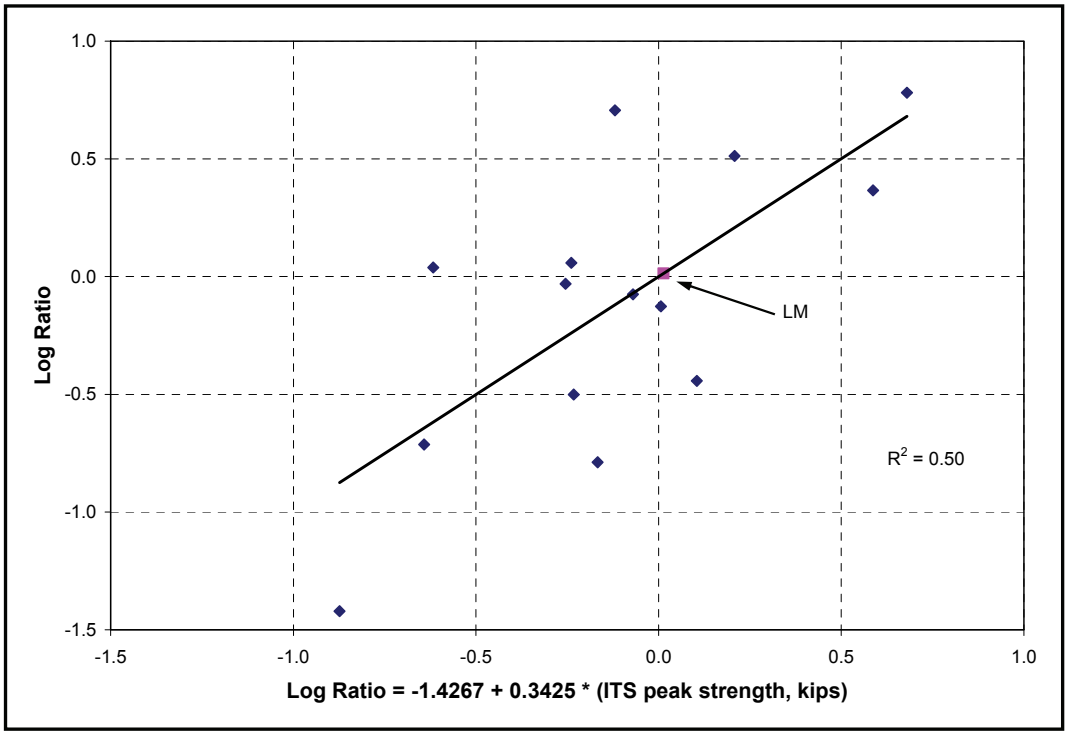

Figure 29. Prediction of Log Ratio using ITS.

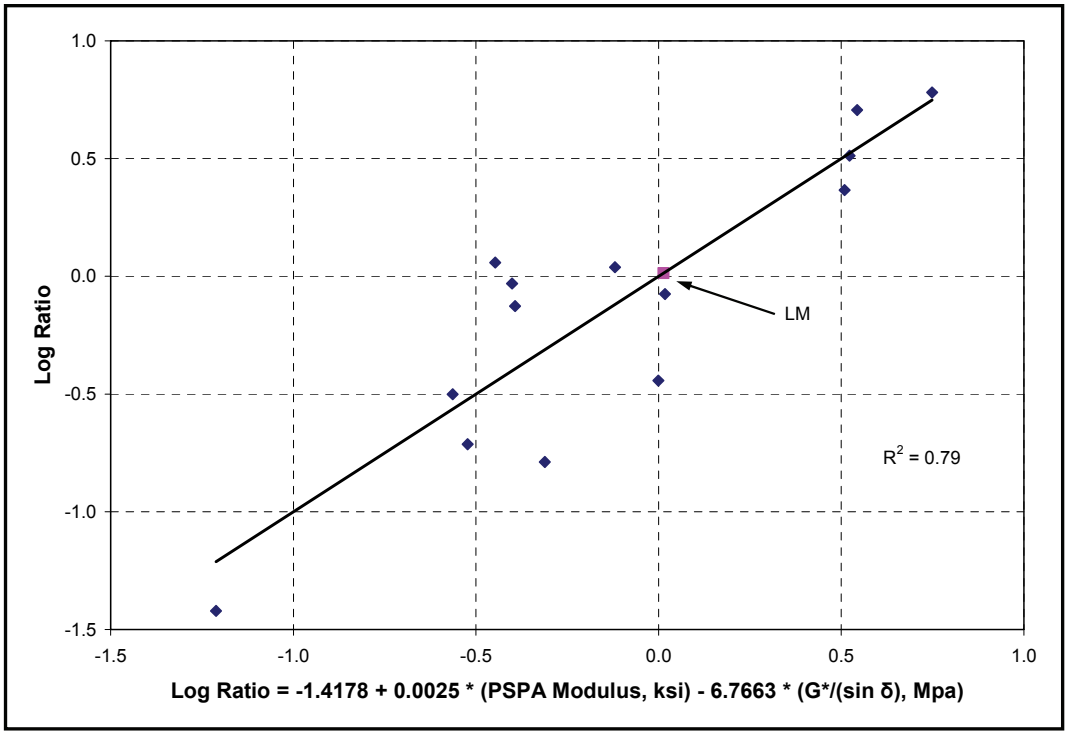

Figure 30. Prediction of Log Ratio using both PSPA modulus and DSR.

Raising both sides of the equation to a power for the number 10:

$$10^{Log\ Ratio} = \frac{measured\ cycles}{predicted\ cycles} \tag{9}$$

Multiplying both sides of the equation by predicted cycles:

$$(predicted\ cycles) * 10^{Log\ Ratio} = measured\ cycles \tag{10}$$

Substituting Equation 3 for predicted cycles:

$$10^{X} * 10^{Log\ Ratio} = measured\ cycles \tag{11}$$

$$X = 2.68\text{-}5.0 * \text{Log}\ S_A - 2.665 * \text{Log}\ E$$

S_A = tensile strain of AC, in./in.
E = elastic modulus of AC, psi

So, for the best estimate of allowable strain repetitions, ε_r, the adjusted criterion would have the form of

$$\varepsilon_r = 10^{(X + Log\ Ratio)} \tag{12}$$

X = $2.68 - 5.0 * \text{Log}\, S_A - 2.665 * \text{Log}\, E$

Log Ratio = represented as one of the regression equations summarized in the last section of the text (Equations 6-8).

For consistency of units between X and *Log Ratio*, the X equation above was changed to allow E in units of kips (force) per square inch.

$$\varepsilon_r = 10^{(X + Log\ Ratio)} \tag{13}$$

X = $-5.315 - 5.0 * \text{Log}\, S_A - 2.665 * \text{Log}\, E$

Log Ratio = represented as one of the regression equations summarized in the last section of the text (Equations 6-8).

If an estimate for modulus is the only data available, the adjusted criterion would be

$$\varepsilon_r = 10^{(X_{aged})} \tag{14}$$

X_{aged} = $-7.1682 - 5.0 * \text{Log}\, S_A - 2.665 * \text{Log}\, E + 0.0028 * E$

S_A = tensile strain of AC, in./in.

E = elastic modulus of AC, ksi

If ITS data are available, the adjusted criterion would be

$$\varepsilon_r = 10^{(X_{aged})} \tag{15}$$

X_{aged} = $-6.7417 - 5.0 * \text{Log}\, S_A - 2.665 * \text{Log}\, E + 0.3425 *$ (*ITS peak*)

S_A = tensile strain of AC, in./in.

E = elastic modulus of AC, ksi

ITS peak = indirect tensile peak strength, kips

If both elastic modulus and $G^*/(\sin \delta)$ are used to modify the criterion for aged AC, the adjusted criterion would be

$$\varepsilon_r = 10^{(X_{aged})} \quad (16)$$

X_{aged} = -6.7328 – 5.0 * Log S_A – 2.665 * Log E + 0.0025 * E -6.7663 * (G*/sin δ)

S_A = tensile strain of AC, in./in.
E = elastic modulus of AC, ksi
G*/(sin δ) = binder stiffness obtained from a DSR, MPa

To establish realistic pavements from which strain response (S_A) could be calculated, several design scenarios were accomplished for C-17, C-130, and F-15 aircraft loads. The tool used for design was the layered elastic approach, as accomplished by the Pavement-Transportation Computer Assisted Structural Engineering (PCASE) software version 2.08 (www.pcase.com). The algorithms in this software adhere to the DoD requirements, as described in the UFC 3-260-02 (Department of Defense 2001). To ensure that the pavements were realistic, the following variable limitations were imposed.

a. All structures consisted of three layers: AC, base course, and subgrade.

b. Elastic modulus for subgrade = 15,000 psi and 30,000 psi.

c. Elastic modulus for base = 50,000 psi and 75,000 psi.

d. Elastic modulus for AC = 350,000 psi and 700,000 psi.

e. AC thickness ≥ 3 in.

f. Single aircraft traffic during pavement life = 2,000 to 1,000,000 repetitions.

The range of pavement types thus designed is shown in Tables 19 and 20.

The same pavement structures were then analyzed under fully loaded C-17, C-130, and F-15 aircraft. Given that the strain response of interest was near the surface of the pavement, each aircraft was simulated as the most heavily loaded single tire. The theoretical analyses assumed that the pavement structures consisted of linear elastic materials with full bond between layers. The pavement structures were assumed to have a stiff

Table 19. Pavement designs and calculated AC strains for a 350-ksi AC modulus.

Aircraft	AC Thickness (in.)	AC Modulus (ksi)	Base Thickness (in.)	Base Modulus (ksi)	Subgrade Modulus (ksi)	Design Passes	S_A
C-17	3	350	19	50	15	2,000	-2.95E-04
C-17	3	350	23	50	15	50,000	-2.94E-04
C-17	3	350	12	75	30	20,000	-1.74E-04
C-17	3	350	14.5	75	30	1,000,000	-1.70E-04
C-17	4	350	17	50	15	2,000	-3.98E-04
C-17	4	350	21.5	50	15	50,000	-3.90E-04
C-17	5	350	15.5	50	15	2,000	-4.36E-04
C-17	5	350	20	50	15	50,000	-4.22E-04
C-17	10.5	350	20	75	30	1,000,000	-2.43E-04
C-130	3	350	13.5	50	15	2,000	-1.83E-04
C-130	3	350	18.5	50	15	200,000	-1.73E-04
C-130	3	350	7.5	75	30	20,000	-1.21E-04
C-130	3	350	10	75	30	1,000,000	-1.03E-04
C-130	4	350	15.5	50	15	50,000	-2.66E-04
C-130	4	350	17	50	15	200,000	-2.62E-04
C-130	4	350	18.5	50	15	1,000,000	-2.59E-04
C-130	5	350	10	50	15	2,000	-3.41E-04
C-130	5	350	15	50	15	200,000	-3.05E-04
C-130	5	350	15.5	50	7.5	2,000	-3.09E-04
C-130	5	350	20	75	30	1,000,000	-1.93E-04
F-15	3	350	16.5	50	15	2,000	-8.92E-04
F-15	3	350	18	50	15	10,000	-8.79E-04
F-15	5	350	20	50	15	20,000	-7.73E-04
F-15	7.5	350	20	50	15	100,000	-5.58E-04
F-15	9	350	20	75	30	1,000,000	-3.66E-04
Analysis based on an AC Poisson's ratio of 0.35, base Poisson's ratio of 0.35, and subgrade Poisson's ratio of 0.40.							

layer with infinite depth beginning at 20 ft below the pavement surface, and the Poisson's ratios for AC, base, and subgrade remained constant as 0.35, 0.35, and 0.40, respectively. The tool used for the linear elastic analyses was software based on Jacob Uzan's Linear Elastic Analysis (JULEA) program. The calculated horizontal strains (S_A) at the bottom of the AC

Table 20. Pavement designs and calculated AC strains for a 700-ksi AC modulus.

Aircraft	AC Thickness (in.)	AC Modulus (ksi)	Base Thickness (in.)	Base Modulus (ksi)	Subgrade Modulus (ksi)	Design Passes	S_A
C-17	3	700	18	50	15	2,000	-3.40E-04
C-17	3	700	22	50	15	50,000	-3.33E-04
C-17	3	700	11	75	30	20,000	-2.35E-04
C-17	3	700	12.5	75	30	200,000	-2.29E-04
C-17	4	700	16	50	15	2,000	-3.85E-04
C-17	4	700	19	50	15	20,000	-3.75E-04
C-17	4	700	9	75	30	20,000	-2.98E-04
C-17	5	700	13.5	50	15	2,000	-3.90E-04
C-17	5	700	16.5	50	15	20,000	-3.75E-04
C-17	12.5	700	20	75	30	1,000,000	-1.52E-04
C-130	3	700	13	50	15	2,000	-2.39E-04
C-130	3	700	19.5	50	15	1,000,000	-2.18E-04
C-130	3	700	6.5	75	30	20,000	-1.86E-04
C-130	3	700	9	75	30	1,000,000	-1.61E-04
C-130	4	700	8	50	15	2,000	-3.35E-04
C-130	4	700	14	50	15	50,000	-2.79E-04
C-130	4	700	15.5	50	15	200,000	-2.73E-04
C-130	4	700	6.5	75	30	500,000	-2.30E-04
C-130	5	700	7.5	50	15	2,000	-3.38E-04
C-130	5	700	13	50	15	200,000	-2.89E-04
C-130	5	700	13.5	50	7.5	2,000	-3.07E-04
C-130	5	700	20	75	30	1,000,000	-1.89E-04
F-15	3	700	15.5	50	15	2,000	-7.64E-04
F-15	5.5	700	20	50	15	20,000	-5.28E-04
F-15	7.5	700	20	50	15	100,000	-3.86E-04
F-15	9.5	700	20	75	30	1,000,000	-2.41E-04
Analysis based on an AC Poisson's ratio of 0.35, base Poisson's ratio of 0.35, and subgrade Poisson's ratio of 0.40.							

layers are included in Tables 19 and 20 and can be used as typical values for Equations 14, 15, and 16. Table 19 shows estimated strain values for an AC modulus of 350 ksi, and Table 20 shows estimated strain values for an AC modulus of 700 ksi.

Evaluating improved accuracy of adjusted fatigue criteria

The results of the beam fatigue tests conducted in this study were predicted with the proposed equations in order to evaluate the three forms of adjusted criteria for aged AC (Equations 14 through 16). Recall that the current DoD criterion was used previously to predict beam fatigue results (Figure 25). Predictions of beam fatigue using the adjusted criterion based on elastic modulus are shown in Figure 31, and predictions of beam fatigue using the adjusted criterion based on ITS are shown in Figure 32. These figures show that while these two criterion adjustments improve the level of conservatism, they do not improve the accuracy of predictions for beam fatigue, relative to Figure 25. Predictions of beam fatigue using the adjusted criterion based on both elastic modulus and G*/(sin δ) are shown in Figure 33. This plot shows both improved conservatism and improved accuracy for beam fatigue predictions, relative to Figure 25.

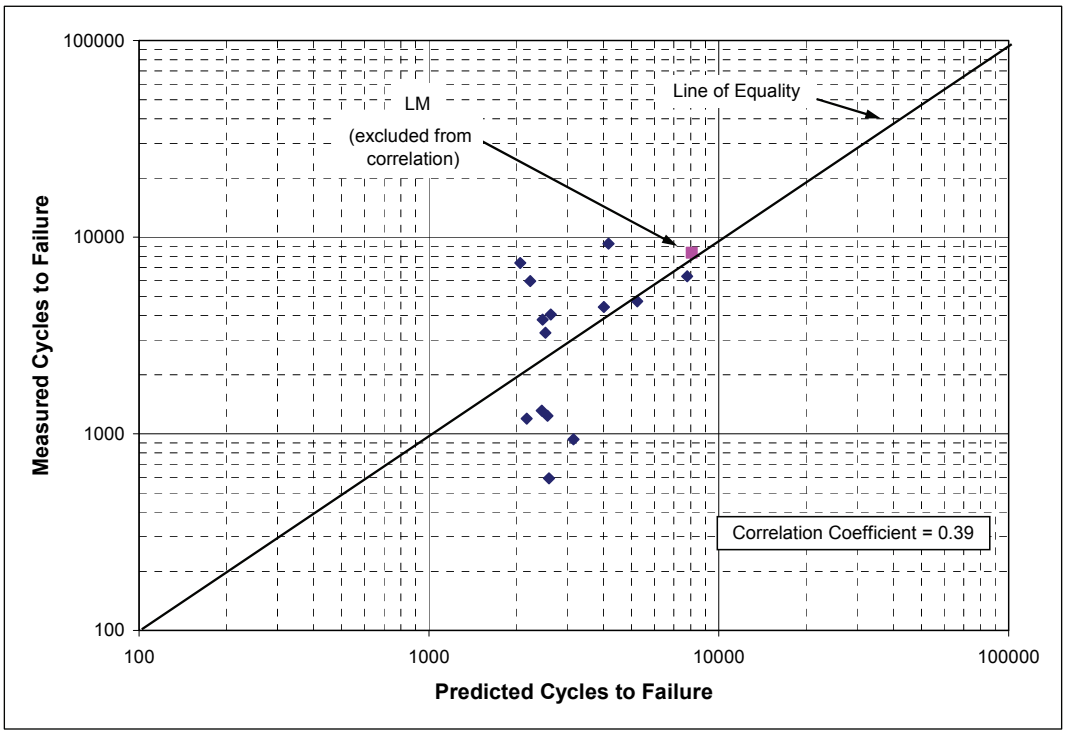

Figure 31. Comparison of predicted and measured cycles to beam fatigue failure where criterion adjustments for aged AC are based on elastic modulus.

Comparisons between Figure 25 and Figures 31 through 33 are summarized in Table 21. Correlation coefficients for the current DoD criterion and the adjusted criterion for aged AC, based on PSPA only and ITS only, were all relatively low. The correlation coefficient for the criterion adjustment using both elastic modulus and G*/(sin δ) was the highest. The average

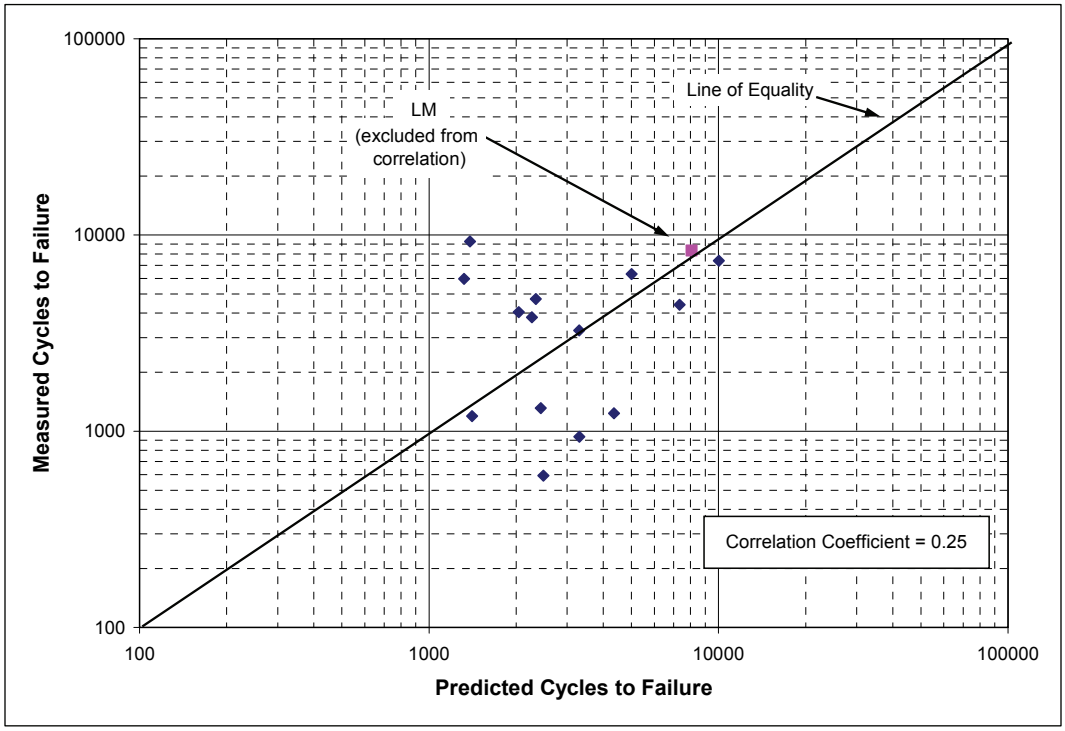

Figure 32. Comparison of predicted and measured cycles to beam fatigue failure where criterion adjustments for aged AC are based on ITS.

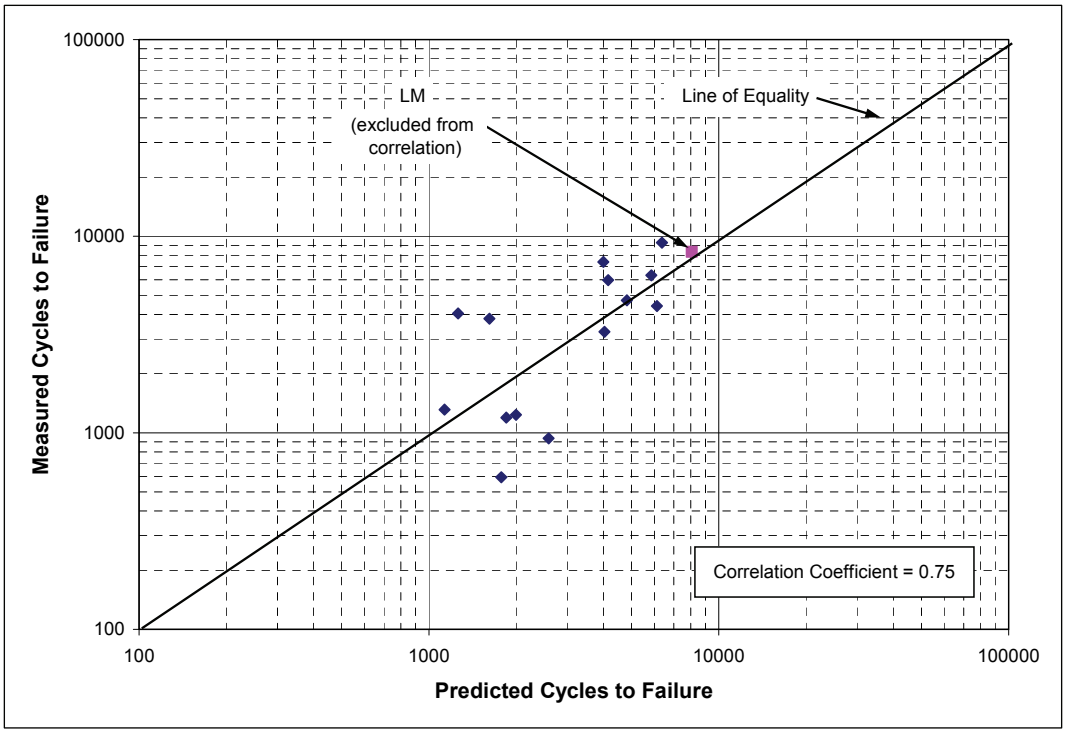

Figure 33. Comparison of predicted and measured cycles to beam fatigue failure where criterion adjustments for aged AC are based on both elastic modulus and G*/(sin δ).

Table 21. Comparisons of predictions for the beam fatigue test results.

Predictor	Correlation Coefficient[a]	Average Deviation[b]	$\sqrt{\sum (deviation)^b}$
Current DoD Criterion (Equation 3 and Figure 25)	-0.27	-1980	33,600
Criterion Adjusted Using Elastic Modulus (Equation 14 and Figure 31)	0.39	600	9,400
Criterion Adjusted Using ITS Peak Strength (Equation 15 and Figure 32)	0.25	670	11,600
Criterion Adjusted Using both Elastic Modulus and G*/(sin δ) (Equation 16 and Figure 33)	0.75	500	6,700
[a] Correlation between predicted cycles to failure and measured cycles to failure. [b] Average of (measured – predicted) cycles to failure.			

deviations in Table 21 reinforce that the adjusted forms of the criterion are conservative, while the current criterion is unconservative on the average for aged AC. The square root of the sum of squared deviations shown in Table 21 reinforces that errors are reduced when predictions are provided by the adjusted forms of the criterion versus the current DoD criterion.

Preliminary design plots for the adjusted fatigue criteria

Recall that Figure 19 provides a graphical representation of the current DoD criterion. Based on the findings in this study, the proposed adjusted forms of the criterion to be used for aged AC can be summarized in similar plots. Plots are shown here for the most promising three forms of criterion adjustment for aged AC:

a. adjustment using elastic modulus

b. adjustment using peak ITS

c. adjustment using both elastic modulus and G*/(sin δ).

The following plots are shown only for the purpose of demonstrating trends and future possibilities. They are not presented as proposed criteria at this time because they are based solely on beam fatigue tests conducted at a single strain level (550 microstrains). The plots are limited to include only the range of test results found in this study. Predictions based on the current DoD criterion are included for comparison purposes.

If elastic modulus is used for the adjusted fatigue criterion, plots would resemble Figures 34 and 35. The two figures show results for two elastic moduli: 300 and 1000 ksi. The figures prove that strain level is the more dominant independent variable compared with elastic modulus; fatigue life decreases with increasing strain. These figures show little influence by elastic modulus. In fact, contrary to the well-documented effects of elastic modulus, Figures 34 and 35 show slightly improved fatigue life for AC with higher elastic moduli. This peculiar characteristic of the figures is attributed to the small number of aged AC samples (14) and to the fact that only two samples measured have elastic moduli greater than 800 ksi. Additional samples are needed to refine these plots. If additional samples do not improve this ambiguity, the fatigue criterion for aged AC could be defined as a function of strain only, thus being independent of elastic modulus. If one compares the adjusted criterion in these figures with the current DoD criterion, it is apparent that the current criterion is underconservative for low moduli and overconservative for high moduli. This point supports the hypothesis that this particular criterion adjustment might be best posed as independent of elastic modulus.

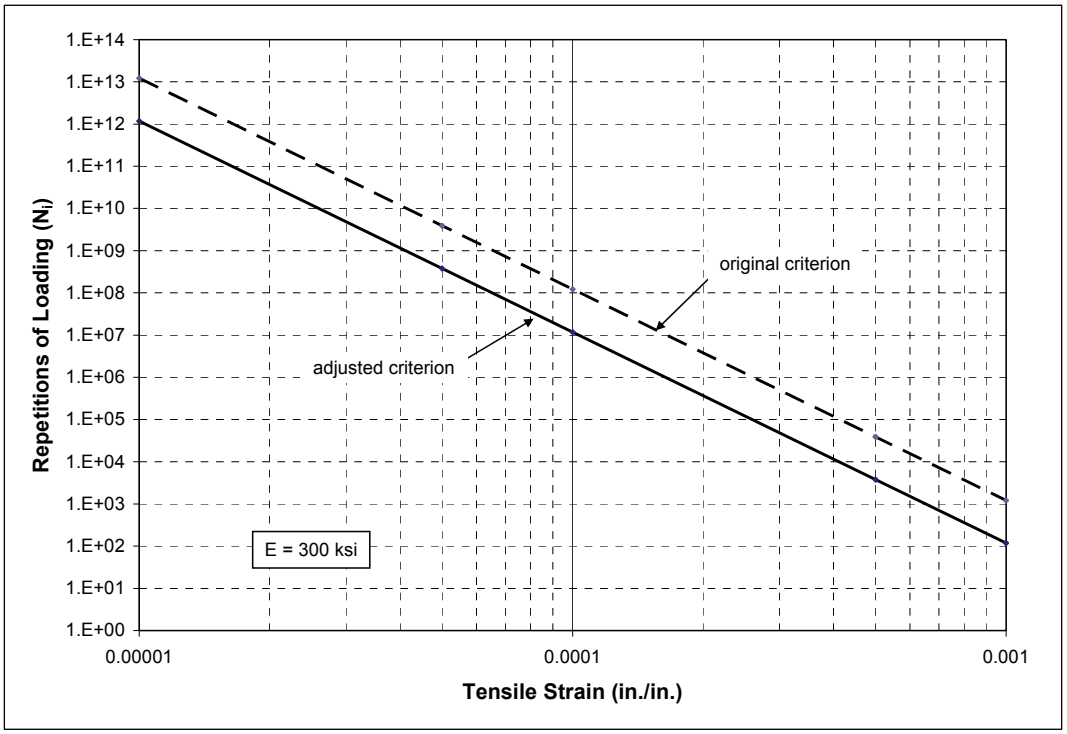

Figure 34. Preliminary adjusted criterion for aged AC with elastic modulus = 300 ksi; criterion adjustment is based solely on elastic modulus.

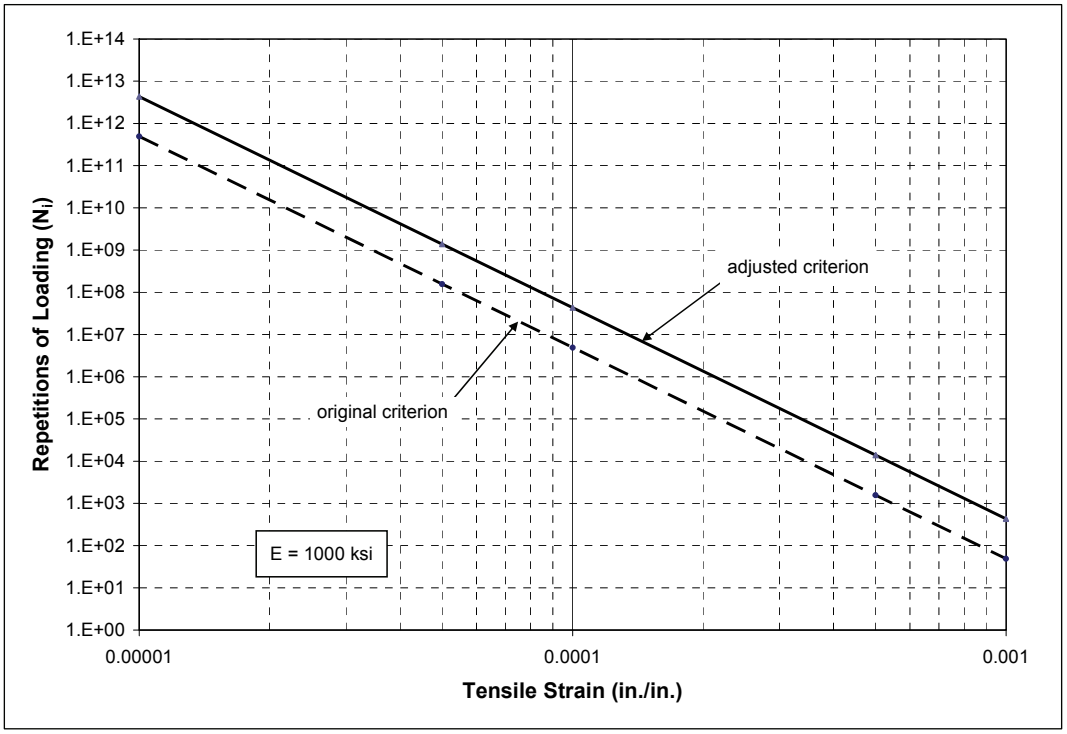

Figure 35. Preliminary adjusted criterion for aged AC with elastic modulus = 1000 ksi; where criterion adjustment is based solely on elastic modulus.

If ITS is used for the adjusted fatigue criterion, plots would resemble Figures 36 and 37. Again, the two figures show results for two elastic moduli: 300 and 1000 ksi. Elastic modulus is still a necessary variable because the adjusted criterion includes the current DoD criterion within its calculation. Strain level is still the dominant independent variable, while ITS and modulus have comparable influences. Fatigue life decreases with increasing strain level, increasing modulus, and decreasing ITS. The adjusted criterion is shown to be similar to the current DoD criterion for ITS values (approximately 4 kips). The current DoD criterion is unconservative for ITS values lower than 4 kips.

If both elastic modulus and $G^*/(\sin \delta)$ are used for the adjusted fatigue criterion, plots would resemble Figures 38 and 39. Strain level is still the dominant independent variable, $G^*/(\sin \delta)$ ranks second in terms of influence, and elastic modulus is nearly inconsequential. This is an important finding given that the combined use of elastic modulus and $G^*/(\sin \delta)$ was shown previously to provide the best prediction for fatigue life. The importance will now be explained. The various forms of criterion adjustments, which were imposed to account for asphalt aging, were developed as correction factors to the current DoD fatigue criterion. Therefore, they

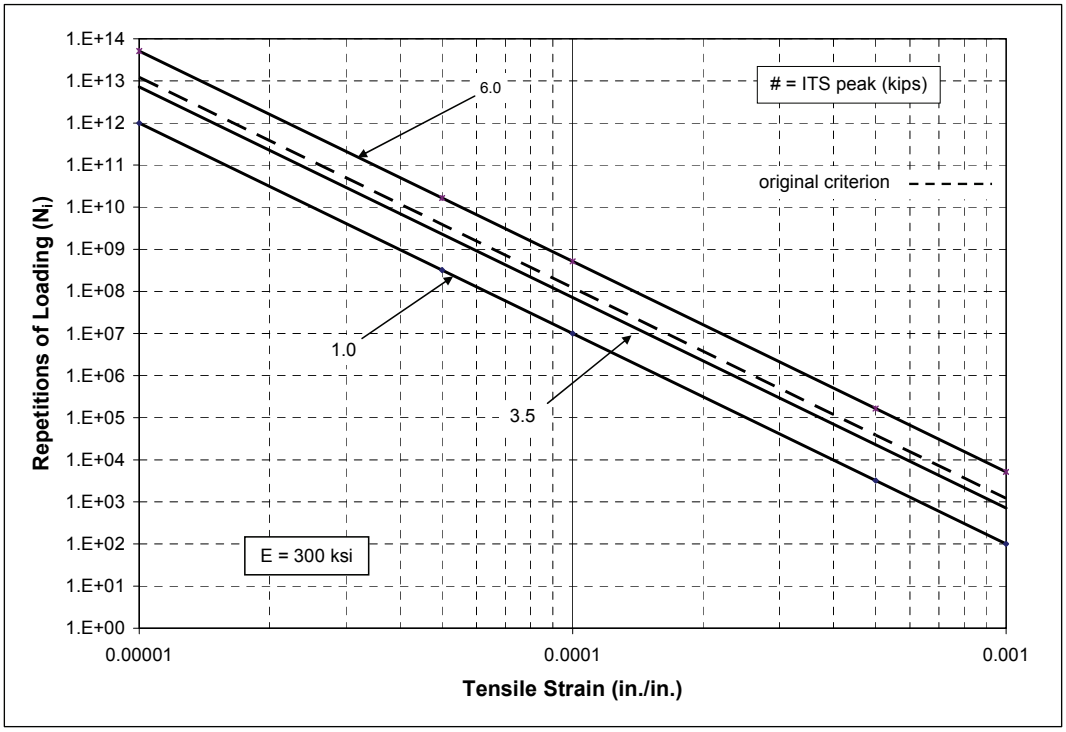

Figure 36. Preliminary adjusted criterion for aged AC with elastic modulus = 300 ksi; where criterion adjustment is based solely on ITS.

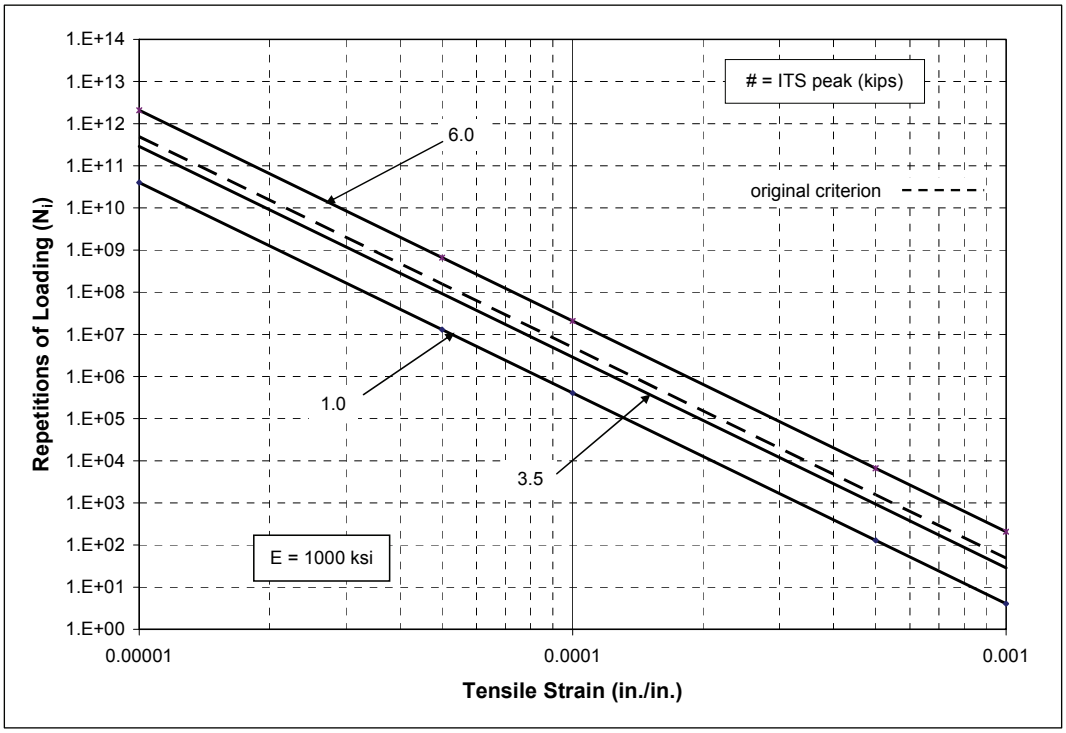

Figure 37. Preliminary adjusted criterion for aged AC with elastic modulus = 1000 ksi; criterion adjustment is based solely on ITS.

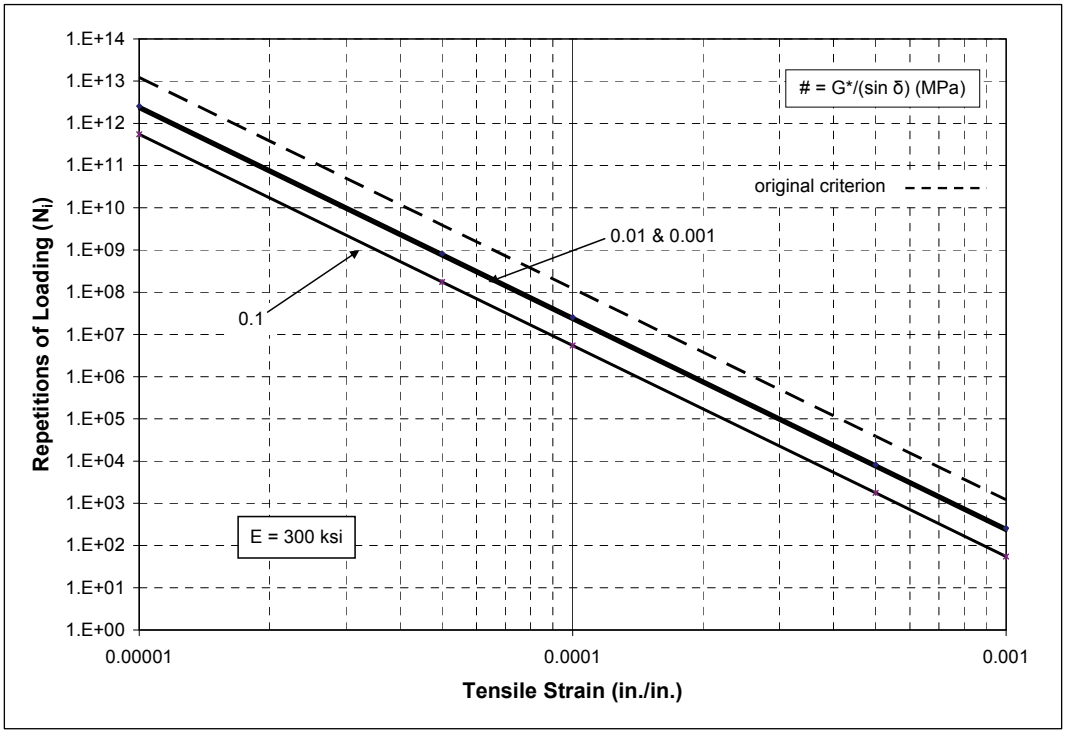

Figure 38. Preliminary adjusted criterion for aged AC with elastic modulus = 300 ksi; criterion adjustment is based on both elastic modulus and G*/(sin δ).

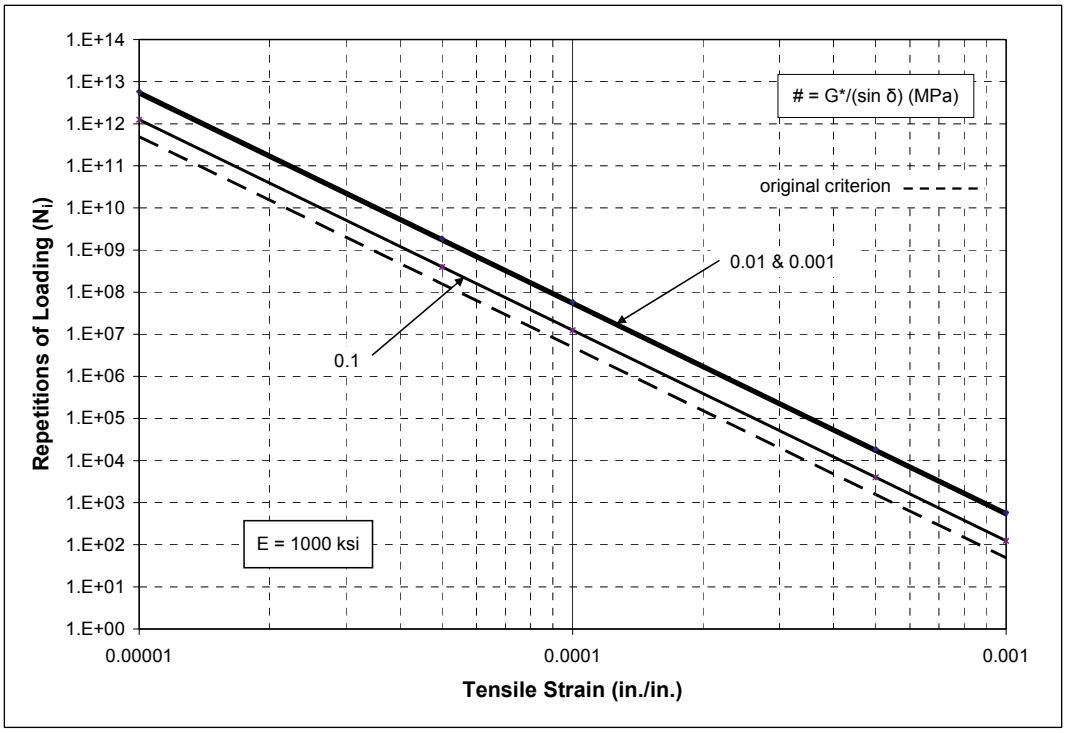

Figure 39. Preliminary adjusted criterion for aged asphalt with elastic modulus = 1000 ksi; criterion adjustment is based on both elastic modulus and G*/(sin δ).

inherently had to include elastic modulus as an independent variable. Figures 38 and 39 show that the best preliminary predictor for fatigue of aged AC essentially minimized the influence of modulus in the fatigue prediction. This finding again supports the hypothesis posed in relation to Figures 34 and 35; that is, future attempts at developing fatigue criteria for aged AC should explore the possibility of eliminating elastic modulus as an independent variable. This can be accomplished only if the current DoD criterion is not used as a developmental starting point. To avoid using the current DoD criterion, the future effort for developing fatigue criteria for aged AC will require beam fatigue testing at various magnitudes of strain.

5 Conclusions and Recommendations

The ERDC was tasked by the AFCESA to develop an evaluation method that accounts for the rapid deterioration of aged AC surfaces. This report addresses the evaluation of aged AC samples from military airfields including field sampling, laboratory testing, and data analysis. Conclusions from the investigation and recommendations for evaluating aged AC pavements are provided in the following text.

Conclusions

The following conclusions resulted from the evaluation of aged AC pavements from February to December 2006:

a. In a laboratory study intended to validate methods by which the PSPA is used for DoD pavement evaluations, the AC design modulus equation (shown below), which is used to adjust the modulus measured by the PSPA to a temperature of 77°F and a standard design frequency of 15 Hz, appears to provide reasonable results for aged AC pavements.

$$E_{77^{o}F} = \frac{E_{PSPA}}{\left(\left\{-0.0109 * \left[(T-32) * \frac{5}{9}\right] + 1.2627\right\} * (3.2)\right)}$$

$E_{77°F}$ = AC design modulus, ksi
E_{PSPA} = modulus measured from the PSPA, ksi
T = AC pavement temperature, °F

b. In the laboratory validation study, PSPA results detected softening of aged AC pavements at a high temperature of 120°F, but did not detect a difference between the moduli of aged AC pavements between the temperatures of 40 and 75°F. This was attributed to the overriding effect of asphalt aging.

c. The current DoD criterion for AC fatigue life, which was developed using laboratory-produced beam samples, predicts fatigue life as a function of AC modulus and tensile strain (or tensile stress). The current DoD criterion has difficulty predicting fatigue failure for aged AC

samples (10+ years) obtained from the field. Results from this study indicate that in some cases the error in this prediction can be highly unconservative; that is, predicted cycles to failure were much higher than measured cycles to failure.

d. A method for adjusting the current DoD fatigue criterion in order to better predict aged AC failure was developed and can be applied to various strain levels and AC moduli. In this study, the developments toward a new criterion were limited to "adjusting" the current criterion because beam fatigue tests were limited to only one strain level (550 microstrains). Results from this study support the need to develop a fatigue criterion for aged AC that is independent of the current DoD criterion. This is best accomplished by conducting beam fatigue tests at various strain levels.

e. AC modulus, as measured by the PSPA, provided the best single material parameter for improving the predictive capability of the current DoD fatigue criterion. AC modulus was found to be an important parameter for "adjusting" the current DoD fatigue criterion because the effect of modulus on fatigue life is diminished for aged AC, relative to its effects for laboratory-produced AC. In other words, modulus was important for the criterion "adjustment" because the net effect of the adjustment was to remove the influence of modulus as an independent predictive variable.

f. The only other material parameter that, when used by itself, offered a significant contribution to adjusting the current DoD fatigue criterion was the peak strength value of the ITS test. This parameter was able to eliminate cases where predicted fatigue life was much higher than measured fatigue life, but overall accuracy of fatigue predictions was not improved substantially. The effectiveness of the ITS parameter was facilitated by its relatively high positive correlation with PSPA modulus.

g. The most preferred method for adjusting the current DoD fatigue criterion involved the use of both PSPA modulus and a viscoelastic binder stiffness property ($G^*/(\sin \delta)$) that was obtained from DSR testing. The authors hypothesize that the effectiveness of this combination is related to the consideration of both mixture and binder properties, as provided by the PSPA and DSR, respectively.

h. AC age, various AC mixture parameters, ITS energy to peak strength, and ITS compression at peak strength showed poor contributions toward adjusting the current DoD AC fatigue criterion, for the purpose of improved predictions of fatigue life for aged AC pavements.

Recommendations

Until further testing and analysis are conducted using varying strain levels, the following recommendations are offered based upon the results of the field and laboratory testing of aged AC pavements:

a. When evaluating aged AC surfaces with the PSPA, use the standard AC design modulus equation (shown below) for converting moduli to "standard" moduli at 77°F and 15 Hz.

$$E_{77^{o}F} = \frac{E_{PSPA}}{\left(\left\{-0.0109 * \left[(T-32) * \frac{5}{9}\right] + 1.2627\right\} * (3.2)\right)}$$

$E_{77°F}$ = AC design modulus, ksi
E_{PSPA} = modulus measured from the PSPA, ksi
T = AC pavement temperature, °F

b. The PSPA can give erroneous results when its contact with the pavement is poor and when surface distresses affect the travel of energy waves. Therefore, the pavement evaluation team needs to ensure that at least three test repetitions are measured at each location and at least ten PSPA measurements are obtained for each pavement feature.

c. Use the following equation to predict aged AC (10+ years) performance if elastic modulus is the only data available:

$$\varepsilon_r = 10^{(X_{aged})}$$

X_{aged} = -7.1682 – 5.0 * Log S_A – 2.665 * Log E + 0.0028 * E

S_A = tensile strain of AC, in./in.
E = elastic modulus of AC, ksi

d. Use the following equation to predict aged AC (10+ years) performance if both elastic modulus and G*/(sin δ) data are available:

$$\varepsilon_r = 10^{(X_{aged})}$$

X_{aged} = -6.7328 – 5.0 * Log S_A – 2.665 * Log E + 0.0025 * E - 6.7663 * (G*/sin δ)

S_A = tensile strain of AC, in./in.
E = elastic modulus of AC, ksi
G*/(sin δ) = binder stiffness obtained from a DSR, MPa

Among the two proposed adjusted criteria, this is the preferred equation because it proved to be the most accurate method for predicting fatigue life in this study.

e. If the strain at the bottom of the AC is unknown, refer to Tables 19 and 20 in Chapter 4 for typical values of S_A based on DoD aircraft, AC thickness, AC modulus, and aircraft pass levels.

References

American Society for Testing and Materials. 2007. *Standard test method for indirect tensile (IDT) strength of bituminous mixtures*. Designation: D 6931-07, West Conshohocken, PA.

Barker, W. R., and W. N. Brabston. 1975. *Development of a structural design procedure for flexible airport pavements*. Report No. FAA-RD-74-199, Federal Aviation Administration. Washington, DC: U.S. Department of Transportation.

Brown, R. E., P. S. Kandhal, T. W. Kennedy, D.-Y. Lee, and F. L. Roberts. 1996. *Hot mix asphalt materials, mixture design, and construction*. 2d ed. Lanham, MD: National Asphalt Pavement Association Research and Education Foundation.

Headquarters, Departments of the Army, the Navy, and the Air Force. 2001a. *Airfield pavement evaluation*. Unified Facilities Criteria (UFC) 3-260-03, Washington, D.C.

Headquarters, Departments of the Army, the Navy, and the Air Force. 2001b. *Pavement design for airfields*. Unified Facilities Criteria (UFC) 3-260-02, Washington, D.C.

Heukelom, W., and A. J. G. Klomp. 1963. Dynamic testing as a means of controlling pavements during and after construction. In *Proceedings, International Conference on the Structural Design of Asphalt Pavements, August 1962*. Ann Arbor, MI: The University of Michigan.

Huang, Y. H. 1993. *Pavement analysis and design*. New York: Prentice Hall.

Kingham, R. I., and B. F. Kallas. 1972. Laboratory fatigue and its relationship to pavement performance. In *Proceedings, Third International Conference on the Structural Design of Asphalt Pavements, September 1972, London England*. Ann Arbor, MI: The University of Michigan.

Nazarian, S., V. Tandon, and D. Yuan. 2005. Mechanistic quality management of asphalt concrete layers with seismic methods. *Journal of ASTM International* 2(8). West Conshohocken, PA: American Society for Testing and Materials.

Nijboer, L. W. 1959. *La Technique Routière*. Vol 4.

Seber, G. A. F. 1977. *Linear regression analysis*. New York: John Wiley and Sons.

Yoder, E. J., and M. W. Witczak. 1975. *Principles of pavement design*. New York: John Wiley and Sons.

Younger, M. S. 1979. *Handbook for linear regression*. Pacific Grove, CA: Duxbury Press.

REPORT DOCUMENTATION PAGE

Form Approved
OMB No. 0704-0188

1. REPORT DATE *(DD-MM-YYYY)*	2. REPORT TYPE	3. DATES COVERED *(From - To)*
June 2007	Final report	

4. TITLE AND SUBTITLE

Evaluation Criteria for Aged Asphalt Concrete Surfaces

5a. CONTRACT NUMBER

5b. GRANT NUMBER

5c. PROGRAM ELEMENT NUMBER

6. AUTHOR(S)

Haley P. Bell and Reed B. Freeman

5d. PROJECT NUMBER

5e. TASK NUMBER

5f. WORK UNIT NUMBER

7. PERFORMING ORGANIZATION NAME(S) AND ADDRESS(ES)

U.S. Army Engineer Research and Development Center
Geotechnical and Structures Laboratory
3909 Halls Ferry Road
Vicksburg, MS 39180-6199

8. PERFORMING ORGANIZATION REPORT NUMBER

ERDC/GSL TR-07-18

9. SPONSORING / MONITORING AGENCY NAME(S) AND ADDRESS(ES)

Headquarters, Air Force Civil Engineer Support Agency
139 Barnes Avenue, Suite 1
Tyndall AFB, FL 32403-5319

10. SPONSOR/MONITOR'S ACRONYM(S)

11. SPONSOR/MONITOR'S REPORT NUMBER(S)

12. DISTRIBUTION / AVAILABILITY STATEMENT

Approved for public release; distribution is unlimited.

13. SUPPLEMENTARY NOTES

14. ABSTRACT

An evaluation of aged asphalt concrete (AC) was performed during the period February to December 2006 at the Vicksburg Airport (Vicksburg, MS), Hood Army Airfield and Robert Gray Army Airfield (Fort Hood, TX), Lawson Army Airfield (Fort Benning, GA), Cairns Army Airfield (Fort Rucker, AL), Butts Army Airfield (Fort Carson, CO), and Kandahar Airfield (Kandahar, Afghanistan) to develop a method for predicting the performance of aged AC surfaces in situ. A portable seismic pavement analyzer (PSPA) was used on the in situ AC pavements to determine the pavement modulus. The aged AC samples obtained from the military airfields were brought to the U.S. Army Engineer Research and Development Center for further laboratory testing. Various asphalt mixture and binder properties were determined from the samples, indirect tensile strength tests were run on core samples, and beam fatigue tests were performed on beam samples. The results from this study were used to develop adjustments to the current Department of Defense (DoD) fatigue criterion for the purpose of improving fatigue life predictions for aged AC surfaces. Aged AC surfaces are considered to be 10 years old or older. The most accurate adjustment to the current DoD criterion required both asphalt modulus (from PSPA) and binder stiffness (from dynamic shear rheometer) as input.

15. SUBJECT TERMS

Asphalt concrete	Department of Defense	Fatigue testing	Modulus
Criteria	Dynamic shear rheometer	Indirect tensile strength	PSPA

16. SECURITY CLASSIFICATION OF:			17. LIMITATION OF ABSTRACT	18. NUMBER OF PAGES	19a. NAME OF RESPONSIBLE PERSON
a. REPORT	b. ABSTRACT	c. THIS PAGE			19b. TELEPHONE NUMBER *(include area code)*
UNCLASSIFIED	UNCLASSIFIED	UNCLASSIFIED		73	